REVIEWS

Architecture and function of metallopeptidase catalytic domains

Núria Cerdà-Costa and Francesc Xavier Gomis-Rüth*

Proteolysis Lab, Department of Structural Biology, Molecular Biology Institute of Barcelona, CSIC, Barcelona, Spain

Received 12 November 2013; Revised 17 November 2013; Accepted 19 November 2013
DOI: 10.1002/pro.2400
Published online 25 November 2013 proteinscience.org

Abstract: The cleavage of peptide bonds by metallopeptidases (MPs) is essential for life. These ubiquitous enzymes participate in all major physiological processes, and so their deregulation leads to diseases ranging from cancer and metastasis, inflammation, and microbial infection to neurological insults and cardiovascular disorders. MPs cleave their substrates without a covalent intermediate in a single-step reaction involving a solvent molecule, a general base/acid, and a mono- or dinuclear catalytic metal site. Most monometallic MPs comprise a short metal-binding motif (HEXXH), which includes two metal-binding histidines and a general base/acid glutamate, and they are grouped into the zincin tribe of MPs. The latter divides mainly into the gluzincin and metzincin clans. Metzincins consist of globular ~130–270-residue catalytic domains, which are usually preceded by N-terminal pro-segments, typically required for folding and latency maintenance. The catalytic domains are often followed by C-terminal domains for substrate recognition and other protein–protein interactions, anchoring to membranes, oligomerization, and compartmentalization. Metzincin catalytic domains consist of a structurally conserved N-terminal subdomain spanning a five-stranded β-sheet, a backing helix, and an active-site helix. The latter contains most of the metal-binding motif, which is here characteristically extended to HEXXHXXGXX(H,D). Downstream C-terminal subdomains are generally shorter, differ more among metzincins, and mainly share a conserved loop—the Met-turn—and a C-terminal helix. The accumulated structural data from more than 300 deposited structures of the 12 currently characterized metzincin families reviewed here provide detailed knowledge of the molecular features of their catalytic domains, help in our understanding of their working mechanisms, and form the basis for the design of novel drugs.

Keywords: structural biochemistry; metzincin clan; catalytic domains; active-site cleft; hydrolytic enzymes; matrix metalloproteases; astacins; ADAM; adamalysins; serralysins; metalloprotease; metalloproteinase

Peptidases

The term "peptidase" is currently recommended for proteolytic enzymes, proteases, and proteinases in general.[1] Peptidases are distributed among all kingdoms of life.[2,3] They target peptide bonds of proteins and/or peptides and some catalyze extensive protein-

Grant sponsor: European Union; Grant number: FP7-HEALTH-2010-261460 "Gums&Joints", FP7-PEOPLE-2011-ITN-290246 "RAPID", and FP7-HEALTH-2012-306029-2 "TRIGGER". Grant sponsor: Spanish Ministries in charge of Science; Grant number: BFU2012-32862 and CSD2006-00015.. Grant sponsor: Fundaciœ "La Marató de TV3; Grant number: 2009-100732. Grant sponsor: Generalitat de Catalunya; Grant number: 2009SGR1036.

*Correspondence to: F. Xavier Gomis-Rüth, Proteolysis Lab, Department of Structural Biology, Molecular Biology Institute of Barcelona, CSIC, Barcelona Science Park, Helix Building, c/Baldiri Reixac, 15–21, E-08028 Barcelona, Spain. E-mail: fxgr@ibmb.csic.es

processing events such as the digestion or degradation of intake proteins and the development, maintenance, and remodeling of tissues. Other peptidases catalyze limited, specific scission of a small number of peptide bonds, which results in the activation or deactivation of themselves and other (pro)enzymes, bioactive peptides, and DNA repressors.[2] In this way, peptidases participate in regulatory mechanisms, which are required in physiological processes such as blood-pressure control, hormone homeostasis, regulation of signal-transduction pathways, and modulation of protein–protein and cell–cell interactions.[4] Such limited proteolysis through "sheddases" produces soluble forms from membrane-anchored precursors, thus decreasing protein concentration at cell surfaces and increasing it in the circulation.[5–7]

Peptidases have traditionally been classified into serine, cysteine, aspartic, and metallopeptidases (MPs) based on elements key for catalysis.[8–10] More recently, three categories have been added: N-terminal threonine peptidases, glutamate peptidases, and asparagine peptidases.[1,11,12] In addition, peptidases are divided into endopeptidases and exopeptidases, which cut in the middle or at the ends of substrates, respectively.[13] The latter, in turn, can be further classified into aminopeptidases and carboxypeptidases, which cleave off N-terminal and C-terminal amino acids, respectively.[1] Overall, exquisite regulation of any proteolytic enzyme is essential for proper functioning and to prevent misdirected temporal and spatial proteolytic activity. Control may be exerted at the transcriptional level or via post-translational modifications. Other regulatory mechanisms include biosynthesis in the form of zymogens that require activation,[14] co-localization of enzyme and substrate, cofactor binding and substrate accessibility and specificity, as well as the presence of physiological protein inhibitors.[15,16] Failure of regulatory mechanisms can give rise to pathologies such as inflammation, tissue destruction (as in arthritis and fibrotic diseases), neurological diseases (Alzheimer's disease, meningitis and multiple sclerosis), and cardiovascular disorders (stroke, hypertension, thrombosis, bleeding, and myocardial infarct).[17–19] Even in tumorigenesis and tumor-progression events, such as angiogenesis, tissue invasion, and metastasis, peptidases play a major role.[20,21] A particular group of peptidases are exogenic virulence factors that lead to the depletion of host defenses and tissue destruction.[22–24] This is observed during microbial infections that cause inflammation, tetanus, pneumonia, tuberculosis, AIDS, malaria, botulism, gas gangrene, bacterial meningitis, anthrax, etc. but also after poisoning after snake bites. Accordingly, such diverse physiopathological implications make these proteins promising drug targets,[25] and their structural studies are thus essential to the understanding of their functional determinants and the design of novel therapeutic agents, now grouped under the term "degradomics."[4,26–29]

Here we review the catalytic domains of MPs, in particular from the metzincin clan.[28,30–37] To date, structures are available for 12 metzincin families: astacins, adamalysins/ADAMs, serralysins, matrixins (*alias* matrix metalloproteinases and MMPs), leishmanolysins, snapalysins, pappalysins, archaemetzincins, fragilysins, cholerilysins, toxilysins, and igalysins (for the first collective mention of the first 10 family names, see Ref. 28).

Classification and Cleavage Mechanism of Metallopeptidases

One widely accepted classification of MPs and proteolytic enzymes in general is provided by the MEROPS database, which classifies homologous sets of peptidases and protein inhibitors hierarchically into protein species, families, and clans based on sequence similarity and evolutionary distances (http://merops.sanger.ac.uk;[38]). This scheme is also followed in a comprehensive study—the *Handbook of Proteolytic Enzymes*.[39] Here, we apply a different approach based on active-site architecture and overall fold similarity (see also Refs. 28, 30, 35, and 40–43). According to this scheme, MPs are first divided into those that have a single catalytic metal and those that have two. Dimetalate MPs mainly include exopeptidases and these are reviewed elsewhere,[44–46] so here we focus on structurally characterized members of the subclass of mononuclear MPs (Fig. 1). In addition, isopeptidases such as Jab1/MPN[47,48] and AMSH-LP deubiquitinases,[49] which cleave amide bonds that are not peptide bonds, and peptide deformylase, which removes N-terminal formyl groups from N-terminal methionine residues,[50,51] have also been omitted. This classification is based on recent structural data and thus supersedes previous reports by our group.[28,43,52]

The active site of MPs accommodates a catalytic divalent metal ion, mostly zinc but also sometimes cobalt, manganese or nickel, which is anchored at the bottom of the active-site cleft of the enzyme by protein residue side chains.[41,53] Here it might be appropriate to clarify commonly used terms that tend to be misused in the literature. The intact, active, metal-bound protein is described as the "enzyme" or the "holoenzyme." If the enzyme has a ligand bound, it can be described as an enzyme–ligand complex. The enzyme lacking a metal ion indispensable for catalysis is described as an "apoenzyme." Metal-binding residues are mostly histidines, aspartates, and glutamates, which are included in zinc-binding motifs that are characteristic of particular MP tribes, clans, and families (Fig. 1, residues in green). Tribes include αβα-exopeptidases, which comprise the funnelin clan;[43,52]

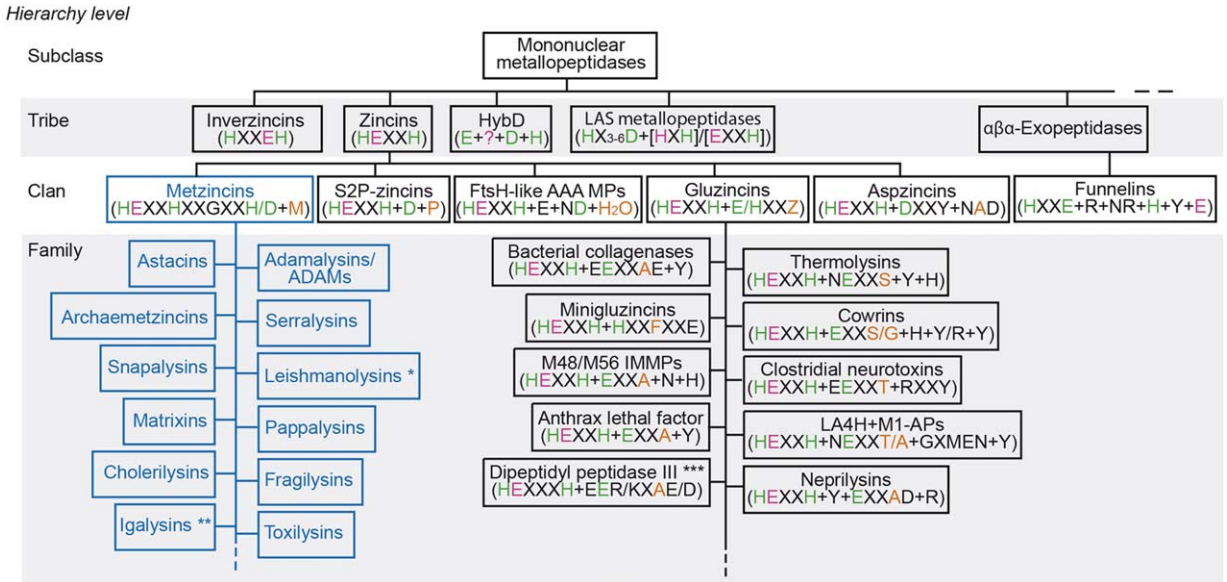

Figure 1. Classification of mononuclear MPs. Within the MP class, mononuclear MPs are a subclass that is divided into tribes currently characterized at the structural level: inverzincins, zincins, relatives of hydrogenase maturating factor (HybD), LAS MPs, and αβα-exopeptidases. These tribes subdivide into clans, which in turn give rise to families. The metzincins are depicted and framed in blue. Metal-binding residues are shown in green, general base/acid residues in magenta, and residues/molecules occupying the position of the Met-turn or Ser/Gly-turn beneath the metal site are in orange. Other residues engaged in substrate binding, stabilization of the reaction intermediate, and/or catalysis are further shown in black, except for X, which stands for any residue and is here only used as a spacer within motifs. Within gluzincins, Z = A/F/S/G/T. Variability within motifs was considered if present only in more than one case. *Leishmanolysins have an extra domain inserted between the glycine and the third histidine metal ligand of the metzincin extended zinc-binding signature. **Igalysins have an extra glycine residue inserted just before the glycine of the metzincin signature. ***Dipeptidyl peptidase III has an extra residue inserted between the general base/acid glutamate and the second metal-binding histidine. This classification supersedes previous schemes.[28,43,52]

LAS MPs;[54–56] relatives of hydrogenase maturating factor, HybD, a proven natural nickel-dependent MP;[57,58] zincins;[30,41,59] and inverzincins.[11,60–62] In all cases, a general/base acid, mostly a glutamate, is further found close to the catalytic metal and is required for catalysis (see the section on "Classification and cleavage mechanism of metallopeptidases" and Fig. 1, residues in magenta).

In general, peptide-bond hydrolysis through monometallic MPs is an ordered single-displacement reaction that follows simple Michaelis-Menten kinetics and occurs optimally at neutral pH. A solvent molecule and a peptide substrate are bound by the active-site cleft and the catalytic metal ion to render the Michaelis complex.[63,64] In most cases, the overall active-site environment is in a competent conformation for catalysis in the mature enzyme before recruiting the peptidic substrate, which binds in extended conformation in such a way that substrate side chains upstream (termed P_1, P_2, P_3, etc.) and downstream (P_1', P_2', P_3', etc.) of the scissile bond nestle into active-site cleft subsites S_1, S_2, S_3, etc. and S_1', S_2', S_3', etc. of the enzyme, respectively.[52,65] In general, substrate specificity is exerted in MPs through S_1'.[52] Cleavage can also occur within protein segments adopting compact tertiary structures, even helical conformations, in the unbound state,[66] as interaction and binding to the peptidase can energetically compensate for substrate unwinding to yield an extended conformation suitable for catalysis.[67] A consensus mechanism for catalysis has been derived after decades of research, mainly on thermolysin from *Bacillus thermoproteolyticus* and bovine carboxypeptidase A,[53,63,68–70] which were the first two MPs to be solved for their crystal structures in the late 1960s and early 1970s,[71,72] and more recently on MMPs.[73,74] This mechanism entails that the solvent molecule is bound first—perhaps it is already part of the mature functional enzyme prior to catalysis as found in the structures of competent MPs in the absence of inhibitors or substrates[74–77]—by the catalytic metal ion and the general base/acid glutamate, which polarizes the solvent and enhances its nucleophilicity (Fig. 2, I). Once the substrate to be cleaved is bound to the cleft, the scissile carbonyl oxygen is bound and polarized by the catalytic metal, and so the carbonyl carbon is more susceptible to nucleophilic attack by the solvent molecule, which simultaneously transfers a proton to the general base glutamate (Fig. 2, II). The catalytic metal thus serves as a dual oxyanion hole and activates both substrates for the reaction. The attack gives rise to a *gem*-diolate tetrahedral reaction intermediate (Fig. 2, III), which

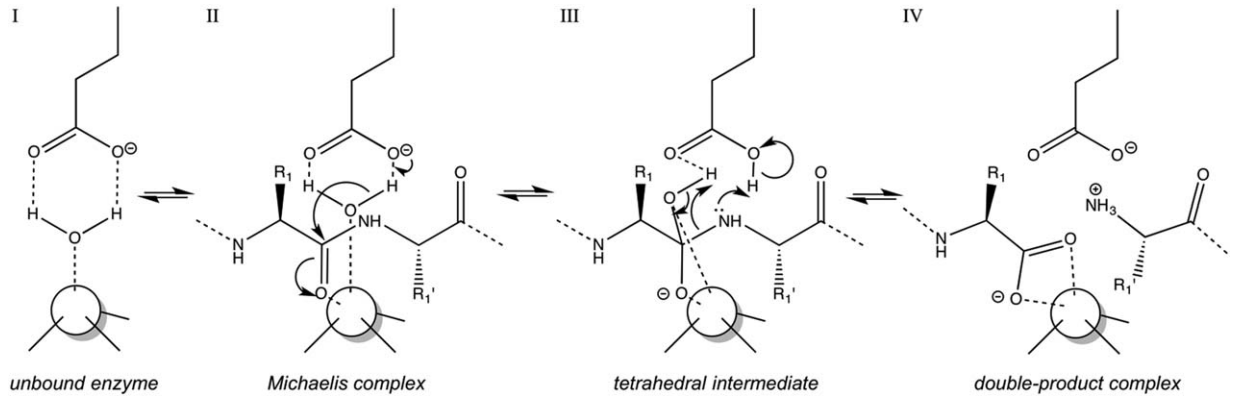

Figure 2. Generally accepted catalytic mechanism of monometallic MPs. The catalytic solvent molecule is bound first to the catalytic metal ion (white sphere) and the general base/acid in the active site in the absence of a peptidic substrate (I). Once the substrate is accommodated in the cleft and the Michaelis complex is formed (II), the polarized solvent molecule attacks the scissile carbonyl group, which leads to the tetrahedral reaction intermediate (III). The latter resolves in scissile bond breakage and double proton transfer to the newly formed α-amino group to render a double-product complex (IV).

is stabilized not only by the metal but also by other protein residues such as vicinal histidines, arginines, and tyrosines[43,53,63] (Fig. 1; see also the section on "Common structural features of metzincins"). Subsequently, the intermediate resolves to the double-product complex through scissile bond cleavage and double proton transfer to the new α-amino terminus (Fig. 2, IV). Finally, the two products dissociate from the enzyme and leave the active-site cleft (the nonprimed product possibly first, see Ref. 53), which is replenished with another solvent molecule and ready for a new round of catalysis.

Zincins Split into Gluzincins and Metzincins

The zincins were named in 1993 by Bode and colleagues.[30] They constitute the most extensive tribe of MPs, with >100 coding genes in humans alone.[59] They have a characteristic short metal-binding amino-acid consensus sequence, HEXXH,[30,41,78] first identified by McKerrow in MMPs and serralysins in 1987,[79] which is provided by an "active-site helix" and supplies two metal-binding histidine ligands and the general base/acid glutamate (see the section on "Classification and cleavage mechanism of metallopeptidases"). In addition, zincins are divided by a horizontal active-site cleft into an upper N-terminal subdomain (NTS) above the cleft and a lower C-terminal subdomain (CTS) below the cleft when viewed in the standard orientation of MPs, i.e., with the peptide substrate running from left to right.[52] The NTS has a helix termed "backing helix" in addition to the active-site helix and a β-sheet of at least three strands, which are mixed parallel/antiparallel. The lowermost strand horizontally frames the top of the active-site cleft, runs antiparallel to a substrate when bound to the cleft, and anchors the latter through inter-main-chain interactions mimicking a β-ribbon. The CTS varies greatly among zincins and is mainly characterized by the presence of a residue (Fig. 1, orange residues) contained in a loop structure providing a basement for the metal-binding site. The two main zincin clans are the gluzincins and the metzincins, whose loop structures are termed, respectively, "Ser/Gly-turn" and "Met-turn" (see below and the section on "Common structural features of metzincins"). Three other zincin clans have an aspartate as third zinc ligand: (i) The S2P-zincins, which include one of the only two integral-membrane MP families structurally characterized to date (those completely imbedded in membranes and not merely type-I or type-II membrane-anchored species); their fold is different from any other zincin, although they have the active-site helix and the short consensus sequence,[52,80] and they show a proline below the metal. (ii) The aspzincins, which were named in 1999 by Ichishima and coworkers[81] in line with the terms gluzincins and metzincins (see below) due to the aspartate metal ligand[81–83] and have an alanine below the metal. (iii) The FtsH-related enzymes, which do not have a protein residue below the metal but rather a solvent molecule.[84–87]

Gluzincins were so named because of a glutamate found as third metal-binding residue, as observed in archetypal thermolysin.[72] The clan name was coined by Hooper in 1994[41] to distinguish the latter enzyme and related structures from the metzincins, which have a histidine instead of the glutamate (see below) and had been named in 1993 by Bode and colleagues based on structural similarities between astacin, adamalysin II and the serralysin *Pseudomonas aeruginosa* alkaline proteinase.[30] Since then, a number of novel MP structures have become available, which has led us to suggest a redefinition of the common structural features of gluzincins: they are zincins, which in addition to their common structural elements contain a "glutamate helix" below the active-site helix, which runs parallel to it in a horizontal projection but is

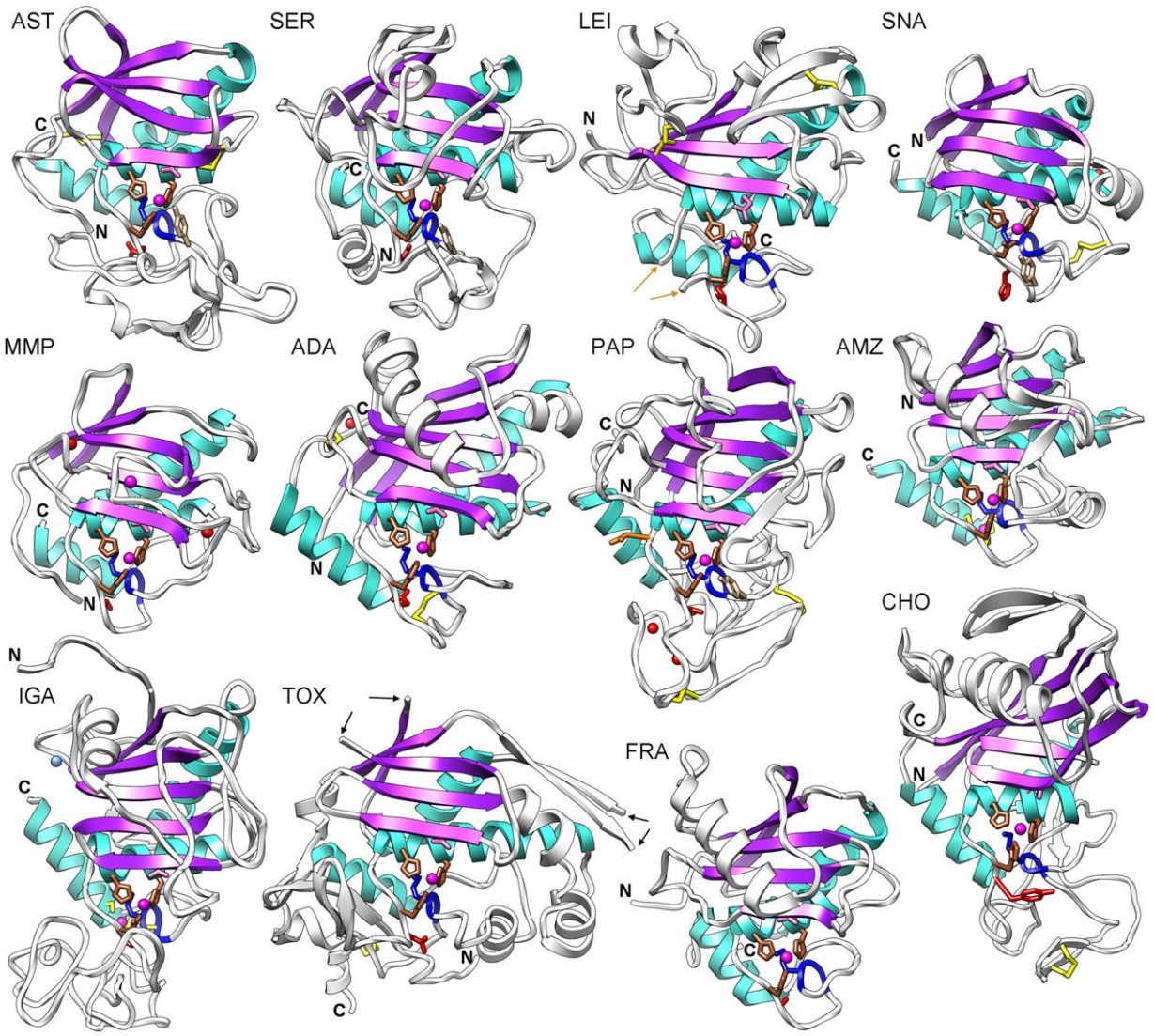

Figure 3. Structure of metzincin catalytic domains. Ribbon-type Richardson plots of a representative member of each of the 12 structurally characterized metzincin families (see the sections on "Common structural features of metzincins" and "Metzincin family-specific features," and Fig. 1) in standard orientation.[52] Depicted are astacin (AST; PDB 1AST; 200 residues), aeruginolysin (SER; PDB 1KAP; 220 residues), leishmanolysin (LEI; PDB 1LML; 213 residues), snapalysin (SNA; PDB 1C7K; 132 residues), human neutrophil collagenase (MMP; PDB 1JAN; 164 residues), adamalysin II (ADA; PDB 1IAG; 203 residues), ulilysin (PAP; PDB 2CKI; 262 residues), *Methanopyrus kandleri* archaemetzincin AmzA (AMZ; PDB 2X7M; 173 residues), igalysin BACOVA_0063 (IGA; PDB 3P1V; 272 residues), toxilysin EcxA (TOX; PDB 4L63; 258 residues), fragilysin-3 (FRA; PDB 3P24; 188 residues), and cholerilysin StcE (CHO; PDB 3UJZ; 258 residues). The common β-strands and α-helices are shown in purple and cyan, respectively (see Fig. 4 for their nomenclature). Unique regular secondary structure elements of each family are in white. The N- and C-termini are labeled and the side chains of the zinc-binding histidines/aspartates (brown), general base/acid glutamates (pink), Met-turn methionines (blue), disulfide-linked cysteines (yellow), family-specific residues (red), and zinc-binding or substrate-stabilizing tyrosines (where present; in tan) are displayed as sticks. Preceding, inserted, and following (sub-)domains have been omitted for clarity. Catalytic metal ions—mostly zinc—are shown as magenta spheres, calcium cations as red spheres, and the potassium cation of IGA is in blue. Orange arrows pinpoint the anchor points for a domain inserted in LEI between the glycine of the extended consensus sequence and the third metal-binding histidine, PAP is unique in having an asparagine instead of the glycine. Black arrows pinpoint two disordered loops in TOX.

rotated backward in a vertical projection (see Fig. 3 in Ref. 43). This helix—or a short loop segment immediately preceding it—provides the third metal-binding residue, mostly a glutamate but sometimes also a histidine as in minigluzincins.[88] This residue is three positions upstream of the residue of the Ser/Gly-turn providing the basement of the metal-binding site[43] (Fig. 1, orange residues). The latter residue varies within gluzincins: it is a phenylalanine in minigluzincins;[88] a threonine in clostridial neurotoxins;[89,90] a serine in thermolysins;[63,72,91–93] and a serine or a glycine in cowrins.[43] However, the most widespread residue among gluzincin families is an alanine as found in anthrax lethal factor and

related proteins such as *Escherichia coli* titration factor Mlc (Mtfa/Yeel);[94,95] in MEROPS M48/M56-family MPs,[38,88] which with human FACE1 and yeast Ste24p are the only other integral-membrane MPs in addition to S2P-zincins structurally analyzed to date;[96,97] in some members—others have a threonine—of the family encompassing leukotriene A4 hydrolase, tricorn interacting factor F3, and MEROPS M1-family aminopeptidases;[98–100] in bacterial collagenases such as those from Clostridium spp.;[101,102] in neprilysins;[103,104] and in dipeptidyl peptidase III and its structural relatives, which uniquely have an additional residue inserted between the signature glutamate and the second histidine, thus resulting in an exceptional HEXXXH signature.[105] This is accounted for by a wider helix turn that allows the second histidine to be suitably positioned to bind the metal ion. Overall, the general hallmark of gluzincins would thus consist of a double consensus motif, HEXXH+(E,H)XX(A,F,T,S,G) (Fig. 1), as well as the minimal structural requirements of zincins plus the presence of a glutamate helix.

In addition to the families reported in Figure 1, other structures show similarities with gluzincins but are probably unable to cleave peptides. Three similar proteins from *Haemophilus influenza*,[106] *Thermotoga maritime*,[107] and *Aquifex aeolicus*[108] possess a gluzincin-like fold but have the catalytic glutamate replaced by a glycine. The structures reported have a third potential histidine metal-ligand but lack a metal at the potential metal-binding site, and no function or catalytic competence has been reported for any of them. By contrast, an endonuclease function in 70S ribosome quality control and 16S rRNA maturation was reported for *Escherichia coli* protein YbeY.[109] This protein shows a structure halfway between a gluzincin and a metzincin despite lacking the general base/acid glutamate—likewise replaced here by a glycine—and may thus be unable to cleave proteins.[110] It bears the extended signature of metzincins (see the section on "Common structural features of metzincins"; the glutamate is replaced by glycine though) and a methionine below the metal-binding site as metzincins do (see the section on "Common structural features of metzincins"), but it also has a glutamate helix as in gluzincins. Actually, YbeY was already identified as a close structural homolog of minigluzincins,[88] placing the latter family also at the interface between gluzincins and metzincins, with a likewise bulky hydrophobic residue in the Ser/Gly-turn, a phenylalanine, and a histidine as third metal ligand instead of the usual glutamate.

Finally, inverzincins,[11,60–62] whose name was also proposed by Hooper in 1994,[41] possess the sequence HXXEH, which is the inverted zincin motif. This led them to be considered a distinct MP tribe (Fig. 1). However, like zincins, they have the motif imbedded within an active-site helix, which runs here characteristically in the opposite direction to the equivalent helix in zincins. In addition, they possess a glutamate helix below the active-site helix, in the same relative position and direction as gluzincins. They have an EXXV motif encompassing the third glutamate metal-binding residue and a valine as the Ser/Ala-turn residue, as well as a mixed β-sheet of at least three strands equivalent to zincins. Furthermore, there is likewise a backing helix in the NTS. Accordingly, although inverzincins are considered a separate tribe from the zincins (Fig. 1), they could also be classified as a special case of gluzincins like the relatives of dipeptidyl peptidase III (see above).

Common Structural Features of Metzincins

Metzincins[28,30–37] are present in all the kingdoms of life and more than 300 structures comprising at least the catalytic domain have been deposited with the Protein Data Bank (PDB; Table I). In the present review, 12 catalytic domain lead structures, one for each of the families depicted in Figure 1, will be discussed (Figs. 3 and 4): *Astacus astacus* crayfish astacin (hereafter AST), *Pseudomonas aeruginosa* alkaline proteinase (*alias* aeruginolysin; SER), *Leishmania major* leishmanolysin (LEI), *Streptomyces caespitosus* neutral protease (*alias* ScNP or snapalysin; SNA), human neutrophil collagenase (*alias* matrix metalloproteinase 8; MMP), *Crotalus adamanteus* snake venom adamalysin II (ADA), the pappalysin ulilysin from *Methanosarcina acetivorans* (PAP), the archaemetzincin AmzA from *Methanopyrus kandleri* (AMZ), the unpublished igalysin "putative MP BACOVA_0063" from *Bacteroides ovatus* (IGA), the toxilysin EcxA from *Escherichia coli* (TOX), fragilysin-3 from *Bacteroides fragilis* (FRA), and the cholerilysin StcE from *Escherichia coli* (CHO)[75,76,111–121]. These prototypes represent archaea, bacteria, protozoa/protists, and eukaryotes. The structures are ~130–270-residue globular moieties that share a common scaffold and active-site environment, with the common elements described for zincins in general (see the section on "Zincins split into gluzincins and metzincins"), but each family has distinguishing structural elements (see the section on "Metzincin family-specific features").

The consensus NTS of metzincins includes a five-stranded twisted β-sheet on the top (Figs. 3–5). All strands (βI to βV) except the fourth are parallel to each other and to any substrate that is bound in the cleft [Fig. 5(a)]. The antiparallel strand, βIV, forms the lower edge of this sub-domain and creates an upper rim or northern wall of the active-site crevice.[122] As discussed for zincins under the section "Zincins split into gluzincins and metzincins," this strand binds a substrate in an antiparallel manner, mainly on its nonprimed side. The loop segment

Table I. *Protein Data Bank Entries Comprising at Least a Metzincin Catalytic Domain (www.pdb.org; Search Completed on October 14, 2013)*

Peptidase name	Organism	PDB access code
ASTACINS		
Astacin	*Astacus astacus*	1ast 1iaa 1iab 1iac 1iad 1iae 1qji 1qjj 3lq0
Tolloid-like protease 1	*Homo sapiens*	3edi
Bone morphogenic protein 1	*H. sapiens*	3edh 3edg
Meprin β	*H. sapiens*	4gwm 4gwn
HCE-1(high choriolyt. enzyme-1)	*Oryzias latipes*	3vtg
ZHE1	*Danio rerio*	3lqb
SERRALYSINS		
Aeruginolysin	*Pseudomonas aeruginosa*	1kap 1jiw 1akl 3vi1
Psychrophilic alkaline protease	*Pseudomonas TACII 18*	1g9k 1h71 1omj 1om6 1om7 1om8 1o0t 1o0q
Serralysin	*Serratia marcescens* / *Serratia* sp. E-15	1af0 1sat 1srp 1smp
PrtC	*Erwinia chrysanthemi*	1go7 1go8 1k7g 1k7i 1k7q 3hb2 3hbu 3hbv 3hda
Psychrophilic marine protease	*Flavobacterium* sp. YS-80-122	3u1r
ADAMALYSINS/ADAMs		
Adamalysin II	*Crotalus adamanteus*	1iag 2aig 3aig 4aig
Atrolysin-C (Ht-d/c)	*Crotalus atrox*	1atl 1dth 1htd
Bothropasin	*Bothrops jararaca*	3dsl
Taiwan habu MP	*Trimeresurus mucrosquamatus*	1kuf 1kug 1kui 1kuk
H_2-proteinase	*Trimeresurus flavoviridis*	1wni
Acutolysin-C	*Agkistrodon acutus*	1qua
Acutolysin-A	*A. acutus*	1bsw 1bud
BaP1	*Bothrops asper*	1nd1 2w12 2w13 2w14 2w15
Vascular apoptosis-inducing protein1 VAP1	*C. atrox*	2ero 2erp 2erq
Fibrin(ogen)olytic MP	*A. acutus*	1yp1
Catrocollastatin/VAP2B	*C. atrox*	2dw0 2dw1 2dw2
Russell's viper venom MP	*Daboia russelli siamensis*	2e3x
BmooMPα-1	*Bothrops moojeni*	3gbo
AaHIV	*A. acutus*	3hdb
Atragin	*Naja atra*	3k7l
K-like MP	*N. atra*	3k7n
TM-1 MP	*T. mucrosquamatus*	4j4m
TNF-α converting enzyme(ADAM-17)	*H. sapiens*	1bkc 3edz 3b92 3cki 2oi0 2i47 2fv9 2fv5 2ddf 2a8h 1zxc 3e8r 3ewj 3g42 3kmc 3kme 3l0t 3l0v 3le9 3lea 3lgp 3o64
ADAM-8	*H. sapiens*	4dd8
ADAM-33	*H. sapiens*	1r54 1r55
ADAMTS-1	*H. sapiens*	2jih 2v4b 3q2g 3q2h
ADAMTS-4	*H. sapiens*	2rjp 3b2z
ADAMTS-5 (alias ADAMTS-11)	*H. sapiens*	3b8z 2rjq 3hy7 3hy9 3hyg 3ljt
MATRIXINS/MMPs		
Fibroblast collagenase (MMP-1)	*H. sapiens*	966c 1ayk 1cge 1cgf 1cgl 1hfc 2ayk 2tcl 3ayk 4ayk 1su3 2j0t 2clt 3shi 4auo
	Sus scrofa	1fbl
Gelatinase A (MMP-2)	*H. sapiens*	1ck7 1hov 1qib 1gxd 1eak 3ayu
Stromelysin-1 (MMP-3)	*H. sapiens*	1b3d 1b8y 1biw 1bm6 1bqo 1c3i 1caq 1ciz 1cqr 3usn 1uea 2d1o 1c8t 2jt6 2jt5 2jnp 1d5j 1d7x 1d8f 1d8m 1g05 1g49 1g4k 1hfs 1hy7 1sln 1slm 1qia 1qic 1ums 1umt 1usn 2srt 2usn 1oo9 3ohl 3oho 4dpe 4g9l 4ja1
Matrilysin (MMP-7)	*H. sapiens*	1mmp 1mmq 1mmr 2ddy 2y6c 2y6d
Neutrophil collagenase (MMP-8)	*H. sapiens*	1jan 1a85 1a86 1bzs 1i73 1i76 1jao 1jap 1jaq 1jh1 1jj9 1kbc 1mmb 1mnc 1zvx 2oy4 1zs0 1zp5 2oy2 3dng 3dpe 3dpf 3tt4

Table I. *Continued*

Peptidase name	Organism	PDB access code
Gelatinase B (MMP-9)	*H. sapiens*	1gkc 1gkd 1l6j 2ow0 2ow1 2ow2 2ovz 2ovx 4h1q 4h2e 4h3x 4h82 4hma
Stromelysin-2 (MMP-10)	*H. sapiens*	1q3a 3v96
Stromelysin-3 (MMP-11)	*Mus musculus*	1hv5
Macrophage elastase (MMP-12)	*H. sapiens*	1jiz 1jk3 2z2d 2k2g 3ba0 2oxu 2oxz 2oxw 2hu6 1z3j 1ycm 1y93 1rmz 1os9 1os2 2poj 1utz 1utt 1ros 2k9c 2krj 2w0d 2wo8 2wo9 2woa 3ehx 3ehy 3f15 3f16 3f17 3f18 3f19 3f1a 3lik 3lil 3lir 3ljg 3lk8 3lka 3n2u 3n2v 3nx7 3rts 3rtt 3ts4 3tsk 3uvc 4efs 4gql 4gr0 4gr3 4gr8 4guy 4h30 4h49 4h76 4h84 4i03 4ijo
Collagenase-3 (MMP-13)	*H. sapiens*	456c 830c 1eub 1fls 1fm1 2pjt 2ozr 2ow9 2e2d 2d1n 1ztq 1you 1xur 1xud 1xuc 2yig 3elm 3i7g 3i7i 3kec 3kej 3kek 3kry 3ljz 3o2x 3tvc 3zxh 4a7b 4fu4 4fvl 4g0d
	M. musculus	1cxv
MT1-MMP (MMP-14)	*H. sapiens*	1bqq 1buv 3ma2
MT3-MMP (MMP-16)	*H. sapiens*	1rm8
Enamelysin (MMP-20)	*H. sapiens*	2jsd
Karilysin	*Tannerella forsythia*	2xs3 2xs4 4in9
SNAPALYSINS		
Neutral protease	*Streptomyces caespitosus*	1c7k 1kuh 4hx3
LEISHMANOLYSINS		
Leishmanolysin	*Leishmania major*	1lml
PAPPALYSINS		
Ulilysin	*Methanosarcina acetivorans*	2cki 2j83 3lum 3lun
ARCHAEMETZINCINS		
AmzA	*Methanopyrus kandleri*	2x7m
	Archaeglobus fulgidus	3zvs 4a3w 4axq
Putative zinc-dependent peptidase	*Methanocorpusculum labreanum*	3lmc
FRAGILYSINS		
Fragilysin-3 (profragilysin-3)	*Bacteroides fragilis*	3p24
CHOLERILYSINS		
StcE	*Escherichia coli O157:H7*	3ujz
TOXILYSINS		
EcxAB toxin	*E. coli*	4l63 4l6t
IGALYSINS		
Putative peptidase BF3526	*B. fragilis*	4df9
Putative metalloendopeptidase BACOVA_0063	*B. ovatus*	3p1v

The primary reference of each structure may be retrieved from the PDB with the respective access code except for coordinates deposited by structural genomics consortia but not published (denoted as "putative").

connecting strands βIII and βIV (LβIIIβIV), the "bulge-edge segment," generates protruding structural elements, which mainly affect subsites S_1' and S_2'. This gives rise to extensive variations in enzyme–substrate interactions on the primed side of the active-site clefts. The NTS also contains a backing helix (αA) and an active-site helix (αB), which are arranged on the concave side of the β-sheet identically in all metzincin structures (Figs. 3–5). Helix αB superimposes well in all structures [Fig. 5(b,c)] and encompasses the first half of the zinc-binding motif, which in metzincins is expanded from HEXXH to HEXXHXXGXX(H,D) and includes the first two zinc-binding histidine residues. At the end of αB, the polypeptide chain takes a sharp, downward turn, mediated by the glycine of the consensus

sequence. The main-chain angles of this residue in the lead structures indicate that any other residue would be in a high-energy conformation and thus disfavored. Pappalysins provide the only notable exception, with an asparagine at this position (see the section on "Pappalysins"). The CSD starts right after this glycine and the chain leads to the third zinc ligand, a histidine or an aspartate, which is the last residue of the metzincin zinc-binding motif and approaches the metal from below [Fig. 5(b,c)]. The residue immediately downstream of the latter is termed the "family-specific residue" and is characteristic for each family. The CSD contains few regular secondary-structure elements, mainly a C-terminal helix (αC) at the end of the polypeptide chain. Helices αB and αC are connected by structures that vary in both length and conformation. However, all structures coincide at a conserved 1,4-β-turn containing a strictly invariant methionine at position three, the Met-turn, which is separated from the third zinc-binding histidine by "connecting segments" ranging from six to 77 amino acids. The methionine is superimposable—including the conformation of its side chain [see Fig. 5(b,c)]—and is positioned underneath the catalytic metal, forming a hydrophobic pillow. However, no contact with the metal is observed. Mutation studies indicated a role for this methionine in the folding and stability of the catalytic domains, although the strict conservation of this residue is still a matter of debate.[123–129] The S_1' pocket of metzincins is the main determinant of substrate specificity and is shaped at the top by the bulge-edge segment and at the bottom by a "wall-forming segment" made up of residues connecting the Met-turn and the C-terminal helix αC.[122] This segment also varies in structure and length, ranging from 9 to 37 residues in the reference structures.

The catalytic zinc ion lies roughly at half width of the active-site cleft at its base. It is coordinated by the Nε2 atoms of the three consensus histidines or two histidine Nε2 atoms and an aspartate Oδ1/2 atom (in SNA and IGA) and the catalytic solvent molecule in an approximately tetrahedral or trigonal pyramidal manner. The solvent molecule is replaced by other ligands in enzyme+inhibitor/product complexes. Some metzincins display a further protein ligand at a slightly greater distance from the catalytic cation in the form of a tyrosine Oη atom, as seen in unbound AST[75] and SER[111] and suggested for unbound PAP.[130] This tyrosine is found two positions downstream of the Met-turn methionine. In SNA and IGA, a tyrosine is found two positions downstream of the metal-binding aspartate, though no longer within binding distance of the catalytic metal ion. The same is observed for the tyrosine found as the family-specific residue in CHO. All these tyrosines may flip back and forth during substrate anchoring, cleavage, and product release, in a motion referred to as the "tyrosine switch" in the particular cases of astacins and serralysins.[131–133] In this, they may play a role in substrate and catalytic-solvent binding and stabilization of the tetrahedral intermediate or the newly created α-amino group of the downstream product.[28,75,131–133] Other, nonconserved residues take over this role in tyrosine-lacking metzincins.

Metzincin Family-Specific Features

Astacins

The first member of the astacin family and first metzincin to be structurally analyzed, in 1992, was the 200-residue digestive crayfish enzyme AST.[75,134] Astacins have disparate biological roles in digestion, development, and tissue remodeling and differentiation—by promoting cartilage and bone formation and collagen biosynthesis—exerted through protein degradation, growth-factor activation, extracellular matrix turnover, and extracellular coat degradation (hatching). Six orthologs are found in humans.[135] The catalytic domain of mature AST is a packman-like ellipsoid and has two sub-domains roughly equal in size (Fig. 3). While the gene of this peptidase encodes only a short pro-peptide, which shields the active-site cleft in the zymogen following an "aspartate-switch" mechanism,[136] and a catalytic MP domain, other family members have additional C-terminal SHK, CUB, LC, TSP, EGF, MAM, TRAF, inserted, transmembrane and cytosolic domains. The astacin family has the longest—together with the families represented by IGA, PAP and CHO—and most sequence-conserved connecting segment among metzincins (see Table I in Ref. 28). The protein scaffold is crosslinked in AST by four conserved cysteine residues forming two disulfide bridges (Fig. 3). The first two residues of the mature enzyme are buried in an internal cavity in the CSD and the N-terminal α-amino group binds the family-conserved residue, a glutamate in astacins. The unbound coordination of the catalytic zinc is trigonal-bipyramidal due to the presence of a fourth invariant, though more distal, tyrosine-switch zinc ligand and the bound (putatively) catalytic solvent molecule (see the section on "Common structural features of metzincins" and Fig. 3). In addition to AST, the structures of mature human tolloid-like protease 1, bone morphogenetic protein 1, meprin β, high choriolytic enzyme 1, and zebrafish hatching enzyme 1, as well as zymogen structures of AST and meprin β, have been reported, totaling 16 structures (see Table I). Reviews and a monograph on the family have been published.[40,135,137–142]

Serralysins

Pathogenic γ-class proteobacterial genera such as Pseudomonas, Erwinia, Serratia, Pectobacterium,

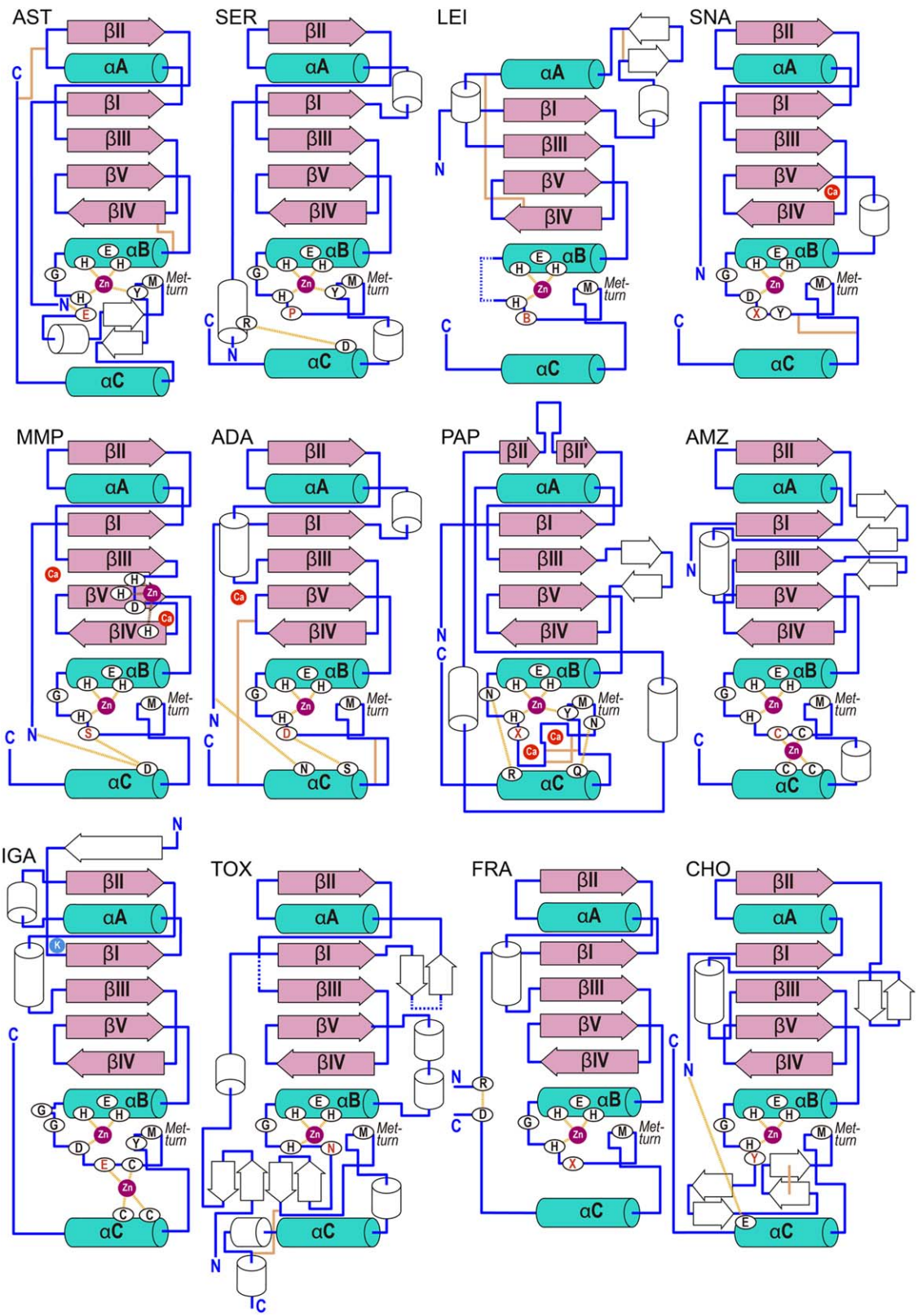

Figure 4. Topology of metzincin catalytic domains. Scheme showing the regular secondary structure elements (helices as rods, strands as arrows) of each metzincin prototype depicted for its structure in Figure 3. The common elements are in pink (strands) and turquoise (helices) and labeled (βI-βV and αA-αC). Hydrogen bonds and metal–ligand bonds are shown as dashed lines, disulfide bonds as orange solid lines. Disordered segments or points of insertion of extra domains are characterized by blue dashes. Family-specific residues are in red, B stands for bulky, hydrophobic residues, X for any residue.

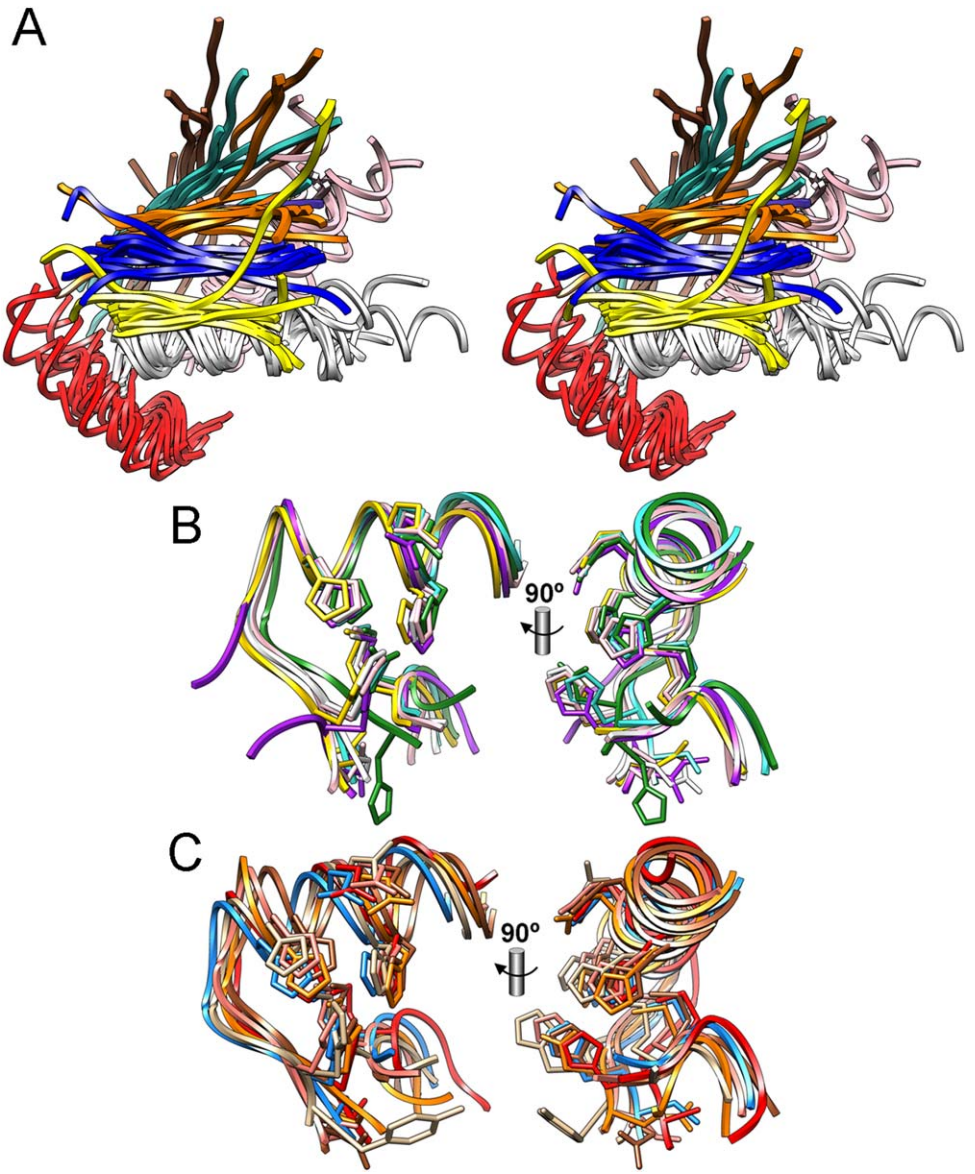

Figure 5. Superposition of common structural elements. (A) Stereo image depicting the superposition of the 12 reference structures only around the common structural elements, β-sheet strands βI (turquoise), βII (brown), βIII (orange), βIV (yellow), and βV (blue), as well as backing helices αA (pink), active-site helices αB (white), and C-terminal helices αC (red). (B) Superposition of the active-site helix and the downstream chain segment until the family-specific residue plus the Met-turn of AST (white), ADA (gold), SER (pink), LEI (purple), MMP (turquoise), and SNA (green) in two orthogonal views. The catalytic metal ions have been omitted for clarity. (C) Same as (B) but showing AMZ (blue), FRA (red), IGA (orange), CHO (tan), PAP (salmon), and TOX (sienna).

Photorhabdus, Morganella, Preoteus, Xenorhabdus, Dickeya, and Yersinia produce ~50-kDa bacterial virulence factors, the serralysins, which are secreted as autoactivatable zymogens.[143,144] Several of these bacteria infect humans and cause—mostly hospital-acquired—infections such as meningitis, endocarditis, pyelonephritis, plague, dermatitis, soft-tissue infections, septicemia, melioidosis, pneumonia, and other respiratory and urinary tract infections. Serralysins are possibly part of the bacterial armamentarium required for such infections, and they have been shown to be active against coagulation factors and defense-oriented proteins, protease inhibitors, lysozyme, and transferrin. They may also trigger an anaphylactic response. The first serralysin to be biochemically and structurally characterized was SER.[111,145,146] Its mature catalytic domain spans 220-residues (Figs. 3 and 4), lacks disulfide bonds, and is followed by a C-terminal β-roll domain stabilized by calcium ions. As in AST, the two SER subdomains are similar in size, and the enzyme starts with a family-specific α-helix in the CSD that is connected with the molecular moiety by a conserved salt bridge with the C-terminal helix αC (Figs. 3 and

4). An elongated LβIαA gives rise to a flap that runs across the convex surface of the β-sheet and differs among serralysins, thus distinctly conditioning substrate binding. The CSD of SER bears an extra α-helix within the wall-forming segment and a second flap shaped by residues of the connecting segment. These elements likewise modulate substrate binding. Comparison of the structures of tetrapeptide-bound SER and that of the unbound ortholog of *Serratia marcescens* reveals that the unliganded zinc coordination is similar to astacin (bipyramidal-trigonal) under inclusion of a tyrosine-switch tyrosine.[147] Further serralysin structures have been reported from *Erwinia chrysanthemi* and *Flavobacterium* sp., totaling 26 (see Table I). Two structures correspond to complexes with cognate protein inhibitors.[148,149]

Leishmanolysins

Leishmanolysins were originally identified as protozoan cell-surface proteins GP63 in trypanosomes, ciliates, and sarcocysts such as those found in the genera Trypanosoma, Leishmania, Crithidia, Naegleria, Tetrahymena, and Sarcocystis. Collectively, these organisms are associated with major human infections such as African trypanosomiasis, meningoencephalitis, Chagas' disease, and leishmaniasis. Leishmanolysins are the major component of the promastigote surface, and they cleave host surface substrates such as CD4 molecules on human T cells. They further protect protozoan promastigotes from inactivation by complement proteins, thus playing a role as virulence factors. Similar sequences to the protozoan forms have been found in mammals (here called invadolysins), insects, plants, fishes, parasitic worms, sponges, mosses, and some bacteria.[28,150] The only structurally analyzed family member is LEI[114](Table I). It is synthesized as a 602-residue inactive precursor in the endoplasmic reticulum provided with a signal peptide and a 100-residue prodomain, which includes a highly conserved cysteine residue potentially acting as a "cysteine switch" (see the section on "Matrixins"). Maturation produces an MP of 276 residues, which includes a 63-residue insertion domain between the glycine and the third metal-binding histidine of the metzincin consensus motif (Figs. 3 and 4), followed by a ~200-residue C-terminal domain. The MP domain is the most asymmetric among metzincins, with a 171-residue NSD and a 42-amino acid CSD, and its N-terminus is found on the back left surface. The NSD has a β-sheet that lacks strand βII (Figs. 3 and 4) and two unique ~40-residue inserted flaps preceding and following backing helix αA, which are linked to the molecular moiety through respective disulfide bonds. A slightly prominent bulge-edge segment preceding strand βIV lies on top of the shallow, medium-sized S_1' pocket, which is framed by the wall-forming segment and active-site helix αB. At the end of the CSD, αC is followed by a segment in extended conformation, which runs parallel across the back surface (Fig. 3 in Ref. 114).

Snapalysins

Streptomyces are predominantly soil bacteria, which collectively produce over two-thirds of the clinically relevant antibiotics in nature. Only few species are pathogenic to humans and may cause mycetoma. SNA is a secreted neutral protease from *Streptomyces caespitosus*, which slowly hydrolyses milk. Similar sequences to SNA have been reported from other Streptomyces species and closely related actinomycetales only. The MP consists of a 132-residue catalytic domain preceded by an alanine-rich 100-amino acid N-terminal extension encompassing a signal-peptide and a pro-domain. SNA thus has the shortest metzincin catalytic domain reported to date and the only three reported PDB entries of the family correspond to *S. caespitosus*, one of them to a heterotetrameric 2 + 2 complex with the dimeric cognate bifunctional protein inhibitor, sermetstatin.[151] The SNA structure is a flattened ellipsoid and is divided into two asymmetric sub-domains.[113,152] It displays all the characteristic metzincin features, connected by short loops, and could therefore represent a minimal metzincin. Particular distinguishing elements are a small LβIIβIII protruding from the upper sheet within the NSD, a small bulge on top of the primed side of the active-site crevice, a short helix in LβVαB, and a calcium-binding site (Figs. 3 and 4). In addition, an aspartate is the third metal-binding protein ligand and, two positions ahead in the sequence, a conserved tyrosine approaches the metal but does not bind it.

Matrixins

Matrixins alias MMPs are secreted or membrane-bound MPs discovered 50 years ago as responsible for tadpole tail resorption during frog metamorphosis.[153] They are found in higher mammals and in animals, plants, and viruses but not in fungi and only in some bacteria, where they do not follow the Darwinian tree-based pathway but may be the result of eukaryotic-to-prokaryotic horizontal gene transfer.[154,155] MMPs exert both broad-spectrum turnover and limited proteolysis of extracellular proteins, which includes ectodomain shedding at the plasma membrane in a complementary fashion to adamalysins/ADAMs (see the section on "Adamalysins/ADAMS"). Substrates include extracellular matrix proteins, peptidases and zymogens, inhibitors, clotting factors, antimicrobial peptides, chemotactic and adhesion molecules, growth factors, hormones, and cytokines, as well as their respective receptors.[156] In these functions, they contribute to physiological actions ranging from tissue processing during embryogenesis and development,

morphogenesis, signaling, and angiogenesis to apoptosis and intestinal defense-protein activation. As a result of this broad spectrum of functions, they play also key roles in pathologies such as inflammation, ulcer, rheumatoid and osteoarthritis, periodontitis, heart failure, atherosclerosis, stroke and cardiovascular disease, fibrosis, emphysema, multiple sclerosis, bacterial meningitis, Alzheimer's disease, HIV-associated dementia, and cancer and metastasis.[157]

Vertebrate MMPs are multimodular proteins consisting of a ~20-residue secretory signal peptide, an ~80-residue pro-peptide, a 160-to-170-residue zinc- and calcium-dependent catalytic domain, a linker region, and a fourfold-propeller hemopexin-like C-terminal domain.[158] Further possible modules include fibronectin type-II-related domains, collagen type-V-like and vitronectin-like insertion domains, cysteine-rich, proline-rich, and interleukin-1 receptor-like domains, immunoglobulin-like domains, glycosyl phosphatidylinositol linkage sequences, membrane anchors and cytoplasmic tails; 23 MMP proteins encoded by 24 genes are found in humans termed MMP-1 to MMP-28 (some numbers are unassigned).[159] Those MMPs encompassing a membrane anchor gave rise to the MT-MMP subfamily.[122,157] MMPs are produced as zymogens that are activated by proteolytic cleavage following a "cysteine switch" or "velcro" mechanism, in which a pro-segment shields access of substrates to the active-site cleft, and a conserved cysteine binds the catalytic metal ion.[160,161] The mature catalytic domain of human neutrophil collagenase (MMP^{112}) is taken here as a prototype (Figs. 3 and 4). Like its orthologs and paralogs, it has a shallow active-site cavity, which separates a larger NSD (~120 residues) from a smaller CSD (~40 amino acids), and a deep hydrophobic S_1' pocket. No disulfide bonds are present in the structure. Characteristically, the N-terminal α-amino group of the mature MP is salt-bridged to the first of two conserved aspartates within helix αC, which also hydrogen-bonds the MMP family-specific residue, a serine or threonine. The NSD displays an S-shaped double loop connecting strands βIII and βIV, which embraces structural zinc and calcium cations. The downstream residues of this segment form a prominent bulge that protrudes into the active-site groove. In addition, LβIVβV and LβIIβIII contribute to a second calcium-binding site on top of the NSD β-sheet (Figs. 3 and 4). In the CSD, MMPs possess the shortest connecting segment within metzincins, with just six to eight residues. MMPs are the most thoroughly studied metzincin family in structural terms, with over 200 structures reported, mostly of MMP-3 and MMP-12 (Table I). These include isolated catalytic domains, multimodular structures and even full-length structures, as well as complexes with their endogenous tissue inhibitors of metalloproteinases (TIMPs), zymogenic structures, and numerous complexes with small-molecule inhibitors. Numerous reviews and monographs have been published and only a few are cited here.[157,162–170]

Adamalysins/ADAMS

The family, termed adamalysins, ADAMs, or reprolysins, has also been the object of extensive studies:[7,171–182] it can be divided into three subgroups, the snake venom MPs, the mammalian ADAMs (19 paralogs in humans), and the likewise mammalian ADAMTSs (19 paralogs in humans). A separate chapter could be dedicated to ADAMDEC1 alias decysin, which has a unique domain structure,[183] and the nine testases, which are ADAMs found only in rodents.[184] The proteins from snake venom cause destruction of extracellular proteins and hemorrhage following bites, while ADAMs were originally discovered in mammalian reproductive tracts engaged in fertilization and sperm function. They are involved in myogenesis, development and neurogenesis, differentiation of osteoblastic cells, cell-migration modulation, and muscle fusion. Due to these critical roles in physiology, they are also related to human disorders such as asthma, cardiac hypertrophy, obesity-associated adipogenesis and cachexia, rheumatoid arthritis, endotoxic shock, inflammation, and Alzheimer's disease. Together with MMPs, (the section on "Matrixins"), they are major contributors to protein ectodomain shedding. Finally, the ADAMTSs disable cell adhesion by binding to integrins. They also participate in gonad formation, embryonic development and angiogenesis, and procollagen activation, as well as in inflammatory processes, cartilage (aggrecan) degradation in arthritic diseases, bleeding disorders, and glioma-tumor invasion.[185]

The family members are extracellular multidomain proteins containing a zinc- and calcium-dependent MP domain. In addition, they can display a pro-domain, C-terminal disintegrin-like, cysteine-rich, C-type lectin, EGF-like, thrombospondin 1-like, and/or transmembrane domains, as well as a cytoplasmic domain. In particular, all mammalian ADAMs are type-I membrane-anchored bitopic proteins, while ADAMTSs lack the transmembrane domain and contain multiple copies of a thrombospondin 1-like repeat and a CUB domain instead, thus being soluble extracellular proteases. Zymogenicity is exerted by pro-domains and activation occurs probably following a cysteine switch-like mechanism as in MMPs (see the section on "Matrixins").[28,160,186] The first structure of a catalytic domain to be solved was that of ADA.[76,187] This is a compact ellipsoidal 203-residue molecule with a relatively flat active-site cleft, which separates a 148-residue NSD from a 54-residue CSD (Figs. 3 and 4). Both the N- and the C-termini are surface located; the former is linked by a hydrogen bond to

the C-terminal helix αC, which also binds the family-specific residue, a glutamate (Fig. 4). ADA deviates from the metzincin consensus due to two additional helices—the one inserted between βII and βIII and running front-to-back is termed "adamalysin helix"—within the NSD. In the CSD, two disulfide-bonds crosslink the irregular connecting segment and attach αC to the NSD, respectively. A calcium ion is located on the surface, opposite the active site and close to the C-terminus (Figs. 3 and 4). The S_1' pocket, characterized by a pronounced bulge-edge segment, is hydrophobic and deep, reminiscent of MMPs.[188,189] In addition to ADA, a number of snake venom MPs, ADAM-8, ADAM-17, ADAM-33, ADAMTS-1, -4, and -5 have been structurally analyzed to date (Table I). These structures include one complex of ADAM-17 with the only endogenous ADAM protein inhibitor reported, TIMP-3.[190]

Pappalysins

This family was named after human PAPP-A alias pappalysin-1, a heavily-glycosylated 170-kDa multi-domain protein specifically cleaving insulin-like growth factor binding proteins,[124] and its paralog pappalysin-2. Closely related sequences are present in mammals, birds, fishes, amphibians, and echinoderms, and somewhat more distant sequences belong to fungi, bacteria, and archaea.[116] Among the latter is 38-kDa PAP from *Methanosarcina acetivorans*, which encompasses only the pro-domain and the catalytic domain.[191] Activation of the PAP zymogen may occur through cysteine-switch as in MMPs (see the section on "Matrixins") as suggested by the presence of a conserved cysteine in the pro-domain. *In vitro*, activation occurs autolytically in the presence of calcium. With 262 residues, mature PAP is the second largest metzincin-prototype catalytic domain and the only family member to be structurally analyzed to date (Table I). As characteristic structural elements, it has a loop dividing strand βII into two substrands (βII and βII'; Figs. 3 and 4), and a β-ribbon inserted within LβIIIβIV that protrudes from the molecular surface and frames the active site on its primed side. The segment connecting αA with βII covers the back of the molecule from the NSD to the CSD in a cape-like fashion and includes two unique α-helices. The glycine of the metzincin zinc-binding motif is exceptionally replaced in PAP and a subset of pappalysins by an asparagine, which binds an arginine within helix αC (Fig. 4). This replacement occurs under slight variation of the main-chain angles, which do not correspond here to a high-energy conformation (see the section on "Common structural features of metzincins") but rather to a left-handed α-helix, although overall, the chain trace is indistinguishable from other metzincins [Fig. 5(b,c)]. The CSD evinces two disulfide bonds and a unique two-calcium site. This site is a molecular switch for activity, as the proteinase can be reversibly inhibited through calcium chelators.[116,130,192] Finally, in the absence of an unbound structure, PAP may possess a fifth zinc-binding tyrosine ligand provided by the Met-turn that is swung out upon substrate binding.

Archaemetzincins

The family name was coined in 2003[28] and the first members to be studied at the biochemical level were the two human orthologs, archaemetzincin-1 and 2, which were reported to hydrolyze synthetic substrates and bioactive peptides.[115] The structures of three archaeal orthologs from *Methanopyrus kandleri*, *Archaeoglobus fulgidus*, and *Methanocorpusculum labreanum* have been reported[118,119] (the latter was only deposited by a structural genomics consortium; see Table I), which however corresponded to inactive species. The family has an extended consensus sequence immediately after the third metal-binding histidine, $CX_4CXMX_{17}CXXC$. This sequence encompasses the Met-turn methionine and four cysteines, which bind a second, structural zinc ion in the CTS below the Met-turn (Figs. 3 and 4) in an element termed the "Cys_4 zinc finger".[118,119] The cysteines are, respectively, in the position of the family-specific residue; two residues ahead of the Met-turn methionine; and in the first and fourth position of the C-terminal helix αC. Moreover, as found in the 175-residue *M. kandleri* protein, AMZ, additional family-characteristic structural elements are an adamalysin helix running front-to-back, two short 3_{10}-helices, a small three-stranded antiparallel β-sheet on the convex side of the NTS β-sheet, and an extra helix within the wall-forming segment in the CTS (Figs. 3 and 4).

Igalysins

This family was not identified in previous sequence-based studies because it does not contain the intact metzincin zinc-binding consensus sequence but has uniquely an additional glycine preceding the signature glcyine and an aspartate as third zinc ligand (HEXXHXXGGXXD) as found in snapalysins (see the section on "Snapalysins"). Only the deposition—but not publication—by a structural genomics consortium of two proteins from *Bacteroides fragilis* and *Bacteroides ovatus* (see Table I), which are thus reported here for the first time, allowed their structural analysis and ascription to the metzincins. These proteins evince significant sequence similarity (BLAST E-values $<10^{-57}$ at www.uniprot.org) with MPs from MEROPS family M64, termed relatives of IgA-peptidase of *Clostridium ramosum*, which cleave prolyl bonds within an *O*-glycosylated, tandemly duplicated octapeptide in the hinge region of human immunoglobulin IgA1.[193,194] These peptidases should not be confused with those of family M26, which groups MPs represented by IgA1-specific

metallopeptidase from *Streptococcus sanguinis*.[38,195,196] Accordingly, the term "igalysins" will be used hereafter to refer to the novel metzincin family of M64 peptidases.

Detailed inspection of *B. ovatus* igalysin (IGA) reveals that, with 272 residues, the structure is the largest reported metzincin catalytic domain, and all the characteristic structural elements for metzincins are observed (Figs. 3 and 4). It shows an asymmetric NTS-CTS tandem (166 and 106 residues, respectively) and, within NTS, on top of the β-sheet, it has an extra sixth β-strand inserted before βI, which runs parallel to the upper-rim strand and antiparallel to the other four. In addition, an adamalysin-helix is inserted between βII and βIII and an extra helix at LαAβII (Fig. 4). The insertion of the extra glycine within the consensus sequence occurs at the end of the active-site helix and is compensated for by the extension of the helix by an additional half turn so that, overall, the chain trace hardly differs from that of the other metzincins [Fig. 5(c)]. As to the CTS, it bears the largest connecting segment (77 residues) but the shortest wall-forming segment (nine residues) within metzincins. As in snapalysin, a tyrosine is found two positions downstream of the third zinc-binding residue—likewise an aspartate—but not within binding distance to the metal. However, the most striking feature is the presence of a second structural metal-binding site within the CTS, which coincides in space with the one found in archaemetzincins (see the section on "Pappalysins") despite completely different chain traces and lengths of the respective connecting segments and wall-forming segments. In IGA, this Cys_4 zinc finger is bound, as in archaemetzincin, by the family-specific residue, which is a glutamate instead of a cysteine; by the first and fourth cysteine residues of the C-terminal helix; and by a cysteine two residues downstream of the Met-turn methionine.

Toxilysins

This is the most recent family, which was discovered while studying bacterial AB_5 toxins.[121] These are virulence factors of pathogenic bacteria that consist of a pentameric B subunit for host-cell invasion and an A subunit that subverts intracellular functions.[197,198] In contrast to previously studied related toxins, EcxAB from *E. coli* and CfxAB from *Citrobacter freundii* exhibit the metzincin consensus sequence within their A subunits, and the crystal structure of the former reveals that they fulfill the structural requirements for a novel metzincin family, the toxilysins.[121,199] The structure of EcxA, the only one reported to date for the family (Table I), is a compact disk of 258 residues (Figs. 3 and 4). The N-terminal segment is extended by ~30 residues preceding NTS strand βI and starts within the CTS. There it contributes with two short strands to a four-stranded antiparallel β-sheet. The N-terminal extension is connected with the Met-turn through a double hydrogen bond formed by the family-specific asparagine with both structural elements. Before entering strand βI and already within the NTS, the polypeptide chain also includes an extra helix. In addition, the NTS bears a β-ribbon within LβIαA and two consecutive helices within LβVαB. Within the CTS, the connecting segment provides two additional strands to the aforementioned extra β-sheet and the wall-forming segment contains an extra helix as found in SER and AMZ (see the sections on "Serralysins" and "Pappalysins"). Finally, the C-terminal segment is also extended beyond αC, adopts a helical conformation in two short stretches, and is linked through a disulfide bond to the protein moiety. The final helix interacts with the pentameric B subunit to yield the AB_5 complex.

Fragilysins

This is the smallest family, with just one member occurring as three closely related isoforms—fragilysin-1, −2, and −3—with 93–96% sequence identity in enteropathogenic *Bacteroides fragilis* (ETBF) only. It was first reported in 1984 as a factor potentially causing acute diarrheal disease in newborn lambs.[200] The chromosomal pathogenicity islet that encodes fragilysins and is absent in nonenterotoxigenic strains contains a second gene, *mpII*, which is countertranscribed and encodes a potential MP of similar size and moderate sequence identity (28–30%) to the three fragilysins. It has recently been shown to be an active MP with a specificity for cleavage between flanking arginines.[201] Fragilysins are the only proven virulence factors of ETBF and target E-cadherin from the intestine of infected mammalian hosts. The structural and function analysis of FRA revealed a 194-residue pro-domain—the largest among metzincins—with unique fold, which plays a major role in protein folding and inhibits the mature 188-residue MP moiety through an aspartate-switch mechanism similarly to astacins (see the section on "Astacins").[117,202] As distinguishing structural features, FRA has an adamalysin helix within the NTS and a characteristic salt bridge that links the N- and the C-terminus at the back of the molecule (Figs. 3 and 4). Overall, the FRA catalytic domain shows remarkable structural similarity with adamalysins/ADAMs despite just ~15% sequence identity (see Supporting Information and Fig. S3b in Ref. 117). Taken together with its restriction to just one protein found in just one organism, this indicates that it may be the result of horizontal gene transfer of an ADAM gene from a mammalian host and subsequent evolution in a bacterial environment, thus giving rise to a unique pro-domain, small structural changes, and a different protein sequence expressed as three isoforms.[117,202]

Cholerilysins

In pathogenic *Vibrio cholerae*, the transmembrane DNA-binding protein ToxR coordinates the expression of essential virulence genes encoded by the *Vibrio* pathogenicity island, including those encoding virulence factors such as the toxin-coregulated type-IV pilus. Among them, ToxR-activated gene A (TagA) lipoprotein has been described.[203] Together with a paralog, another protein from *Burholderia*, and protein StcE (secreted protease of C1-esterase inhibitor; CHO), they were proposed in 2003 to constitute the cholerilysin family,[28] which coincides with MEROPS family M66[38] and the SLiMe family.[204,205] CHO is an 898-residue virulence factor secreted by enterohemorrhagic *E. coli*. It acts as a mucinase hydrolyzing glycoproteins of the mucosal barrier that lines and protects the mammalian gastrointestinal tract, thus contributing to bacterial penetration during infection.[206] CHO includes a central 258-residue catalytic domain flanked upstream by two immunoglobulin-like domains and an insertion region and downstream by two disordered regions and a C-terminal domain.[120] This is the only structure reported for the family (Table I): it is shaped like a banana, while comprising all the structural hallmarks of metzincins. However, in comparison with other metzincins, CHO shows an unusually open active-site cleft, which is compatible with binding of large *O*-glycosylated substrates.[120] In addition, it features a helix on the convex face of the NTS β-sheet, in a similar position though different orientation to the adamalysin helix of other metzincins. Furthermore, an active-site flap with a short β-ribbon is inserted after strand βII, which replaces the bulge-edge segment in other metzincins in shaping the active-site cleft top on its primed side. Between the family-specific tyrosine, which points toward the bulk solvent in the reported structure but could belong to a tyrosine switch (see the section on "Common structural features of metzincins"), and the Met-turn, two additional β-ribbons are found within the CTS; the first contains a conserved sequence, WGWD,[205] and the second is crosslinked by a disulfide bond. Finally, the N-terminal α-amino nitrogen is linked through a salt bridge with a glutamate in the penultimate position of the C-terminal helix αC, five residues upstream of the catalytic domain C-terminus.

Concluding Remarks

The metzincins are ubiquitous MPs that participate in pathophysiological metabolic processes. Twelve metzincin families have been characterized at the structural level, some are restricted to certain taxa, others span several kingdoms, and even others are most likely the product of horizontal gene transfer. In addition to those structurally characterized, several more families may enlarge the clan based on the presence of the characteristic extended zinc-binding consensus sequence pattern and its small variants as found in some current family members. The structural evidence, accumulated over the past 21 years, has enabled us to confirm the hypothesis proposed in 1993 that they share a set of characteristic structural elements and a catalytic metal environment despite negligible overall sequence similarity. Accordingly, this MP clan can be envisaged as an example of divergent evolution since the onset of life—they are present in archaea—from an archetypal minimal *urmetzincin*, which may have spanned ~100–110 residues and may not have looked very different from the smallest current member, 132-residue snapalysin. Within this initial scaffold, functional requirements and the associated evolutionary processes would have led to the introduction of specific structural elements, which eventually resulted in the distinct current families. The structural information reviewed here may help to ascribe the function of proteins encoded by newly discovered gene sequences and in the elucidation of common catalytic mechanisms but also of their detailed differences, which may enable the design of specific and selective inhibitors and activators to modulate their activity.

Acknowledgments

Ulrich Baumann and Johann (Hans) Brandstetter are warmly thanked for critical reading of the manuscript, as is Robin Rycroft. This study was supported in part by grants from European, Spanish, and Catalan agencies.

References

1. Barrett AJ, Rawlings ND, Salvesen G, Woessner JF. Introduction. In: Rawlings ND, Salvesen G, Eds. (2013) Handbook of proteolytic enzymes. Oxford (UK): Academic Press, pp Ii–Iiv.
2. Neurath H. Limited proteolysis and zymogen activation. In: Reich E, Rifkins DB, Shaw E, Eds. (1975) Proteases and biological control. New York: Cold Spring Harbor Laboratory Press, pp 51–64.
3. Neurath H, Walsh KA (1976) Role of proteolytic enzymes in biological regulation. Proc Natl Acad Sci USA 73:3825–3832.
4. López-Otín C, Overall CM (2002) Protease degradomics: a new challenge for proteomics. Nat Rev Mol Cell Biol 3:509–519.
5. Kheradmand F, Werb Z (2002) Shedding light on sheddases: role in growth and development. BioEssays 24:8–12.
6. Arribas J, Merlos-Suárez A (2003) Shedding of plasma membrane proteins. Curr Top Dev Biol 54:125–144.
7. Blobel CP (2005) ADAMs: key components in EGFR signalling and development. Nat Rev Mol Cell Biol 6: 32–43.
8. Hartley BS (1955) Chemical nature of the active centres of enzymes. Ann Repts Prog Chem 51:303–311.

9. Hartley BS (1960) Proteolytic enzymes. Ann Rev Biochem 29:45–72.
10. Barrett AJ, McDonald JK (1986) Nomenclature: protease, proteinase and peptidase. Biochem J 237:935–935.
11. Rawlings ND, Barrett AJ, Bateman A (2010) MEROPS: the peptidase database. Nucleic Acids Res 38: D227–D233.
12. Rawlings ND, Barrett AJ, Bateman A (2011) Asparagine peptide lyases: a seventh catalytic type of proteolytic enzymes. J Biol Chem 286:38321–38328.
13. Barrett AJ, Rawlings ND, Woessner JF (2004) Handbook of proteolytic enzymes. Amsterdam: Elsevier.
14. Stroud RM, Kossiakoff AA, Chambers JL (1977) Mechanisms of zymogen activation. Annu Rev Biophys Bioeng 6:177–193.
15. Holzer H, Heinrich PC (1980) Control of proteolysis. Annu Rev Biochem 49:63–91.
16. Rawlings ND, Tolle DP, Barrett AJ (2004) Evolutionary families of peptidase inhibitors. Biochem J 378:705–716.
17. Dollery CM, Libby P (2006) Atherosclerosis and proteinase activation. Cardiovasc Res 69:625–635.
18. Murphy G, Nagase H (2008) Reappraising metalloproteinases in rheumatoid arthritis and osteoarthritis: destruction or repair? Nat Clin Pract Rheumatol 4: 128–135.
19. Nalivaeva NN, Fisk LR, Belyaev ND, Turner AJ (2008) Amyloid-degrading enzymes as therapeutic targets in Alzheimer's disease. Curr Alzheimer Res 5: 212–224.
20. Chang C, Werb Z (2001) The many faces of metalloproteases: cell growth, invasion, angiogenesis and metastasis. Trends Cell Biol 11:S37–43.
21. López-Otín C, Matrisian LM (2007) Emerging roles of proteases in tumour suppression. Nat Rev Cancer 7: 800–808.
22. Miyoshi S, Shinoda S (2000) Microbial metalloproteases and pathogenesis. Microbes Infect 2:91–98.
23. Taylor LH, Latham SM, Woolhouse ME (2001) Risk factors for human disease emergence. Phil Trans Royal Soc London B 356:983–989.
24. Potempa J, Pike RN (2005) Bacterial peptidases. Contrib Microbiol 12:132–180.
25. Turk B (2006) Targeting proteases: successes, failures and future prospects. Nat Rev Drug Discov 5:785–799.
26. Bjarnason JB, Fox JB (1994) Hemorrhagic metalloproteinases from snake venoms. Pharmac Ther 62:325–372.
27. Tonello F, Morante S, Rossetto O, Schiavo G, Montecucco C (1996) Tetanus and botulism neurotoxins: a novel group of zinc-endopeptidases. Adv Exp Med Biol 389:251–260.
28. Gomis-Rüth FX (2003) Structural aspects of the metzincin clan of metalloendopeptidases. Mol Biotech 24: 157–202.
29. Quesada V, Ordoñez GR, Sánchez LM, Puente XS, López-Otn C (2009) The Degradome database: mammalian proteases and diseases of proteolysis. Nucleic Acids Res 37:D239–D243.
30. Bode W, Gomis-Rüth FX, Stöcker W (1993) Astacins, serralysins, snake venom and matrix metalloproteinases exhibit identical zinc-binding environments (HEXXHXXGXXH and Met-turn) and topologies and should be grouped into a common family, the 'metzincins'. FEBS Lett 331:134–140.
31. Stöcker W, Bode W (1995) Structural features of a superfamily of zinc-endopeptidases: the metzincins. Curr Opin Struct Biol 5:383–390.
32. Stöcker W, Grams F, Baumann U, Reinemer P, Gomis-Rüth FX, McKay DB, Bode W (1995) The metzincins—Topological and sequential relations between the astacins, adamalysins, serralysins, and matrixins (collagenases) define a superfamily of zinc-peptidases. Prot Sci 4:823–840.
33. Bode W, Grams F, Reinemer P, Gomis-Rüth FX, Baumann U, McKay DB, Stöcker W (1996) The metzincin-superfamily of zinc-peptidases. Adv Exp Med Biol 389:1–11.
34. Sterchi EE (2008) Special issue: metzincin metalloproteinases. Mol Aspects Med 29:255–257.
35. Gomis-Rüth FX (2009) Catalytic domain architecture of metzincin metalloproteases. J Biol Chem 284: 15353–15357.
36. Rivera S, Khrestchatisky M, Kaczmarek L, Rosenberg GA, Jaworski DM (2010) Metzincin proteases and their inhibitors: foes or friends in nervous system physiology? J Neurosci 30:15337–15357.
37. Balaban NP, Rudakova NL, Sharipova MR (2012) Structural and functional characteristics and properties of metzincins. Biochem Biokhim 77:119–127.
38. Rawlings ND, Barrett AJ, Bateman A (2012) MEROPS: the database of proteolytic enzymes, their substrates and inhibitors. Nucleic Acids Res 40:D343–D350.
39. Rawlings ND, Salvesen G (2013) Handbook of proteolytic enzymes. Oxford (UK): Academic Press, pp 4094.
40. Jiang W, Bond JS (1992) Families of metalloendopeptidases and their relationships. FEBS Lett 312:110–114.
41. Hooper NM (1994) Families of zinc metalloproteases. FEBS Lett 354:1–6.
42. Lewis AP, Thomas PJ (1999) A novel clan of zinc metallopeptidases with possible intramembrane cleavage properties. Prot Sci 8:439–442.
43. Gomis-Rüth FX (2008) Structure and mechanism of metallocarboxypeptidases. Crit Rev Biochem Mol Biol 43:319–345.
44. Lowther WT, Matthews BW (2002) Metalloaminopeptidases: common functional themes in disparate structural surroundings. Chem Rev 102:4581–4608.
45. Seibert CM, Raushel FM (2005) Structural and catalytic diversity within the amidohydrolase superfamily. Biochemistry 44:6383–6391.
46. Botelho TO, Guevara T, Marrero A, Arêde P, Fluxa VS, Reymond JL, Oliveira DC, Gomis-Rüth FX (2011) Structural and functional analyses reveal that Staphylococcus aureus antibiotic resistance factor HmrA is a zinc-dependent endopeptidase. J Biol Chem 286:25697–25709.
47. Tran HJ, Allen MD, Lowe J, Bycroft M (2003) Structure of the Jab1/MPN domain and its implications for proteasome function. Biochemistry 42:11460–11465.
48. Ambroggio XI, Rees DC, Deshaies RJ (2004) JAMM: a metalloprotease-like zinc site in the proteasome and signalosome. PLoS Biol 2:E2.
49. Sato Y, Yoshikawa A, Yamagata A, Mimura H, Yamashita M, Ookata K, Nureki O, Iwai K, Komada M, Fukai S (2008) Structural basis for specific cleavage of Lys 63-linked polyubiquitin chains. Nature 455:358–362.
50. Meinnel T, Blanquet S, Dardel F (1996) A new subclass of the zinc metalloproteases superfamily revealed by the solution structure of peptide deformylase. J Mol Biol 262:375–386.
51. Chan MK, Gong W, Rajagopalan PT, Hao B, Tsai CM, Pei D (1997) Crystal structure of the Escherichia coli peptide deformylase. Biochemistry 36:13904–13909.

52. Gomis-Rüth FX, Botelho TO, Bode W (2012) A standard orientation for metallopeptidases. Biochim Biophys Acta 1824:157–163.
53. Auld DS. Chapter 78—Catalytic mechanism for metallopeptidases. In: Rawlings ND, Salvesen G, Eds. (2013) Handbook of proteolytic enzymes. Oxford: Academic Press, pp 370–396.
54. Bochtler M, Odintsov SG, Marcyjaniak M, Sabala I (2004) Similar active sites in lysostaphins and D-Ala-D-Ala metallopeptidases. Prot Sci 13:854–861.
55. Marcyjaniak M, Odintsov SG, Sabala I, Bochtler M (2004) Peptidoglycan amidase MepA is a LAS metallopeptidase. J Biol Chem 279:43982–43989.
56. van Heijenoort J (2011) Peptidoglycan hydrolases of Escherichia coli. Microbiol Mol Biol Rev: MMBR 75:636–663.
57. Fritsche E, Paschos A, Beisel HG, Bock A, Huber R (1999) Crystal structure of the hydrogenase maturating endopeptidase HYBD from Escherichia coli. J Mol Biol 288:989–998.
58. Theodoratou E, Huber R, Bock A (2005) [NiFe]-Hydrogenase maturation endopeptidase: structure and function. Biochem Soc Trans 33:108–111.
59. Lenart A, Dudkiewicz M, Grynberg M, Pawlowski K (2013) CLCAs—A family of metalloproteases of intriguing phylogenetic distribution and with cases of substituted catalytic sites. PloS One 8:e62272.
60. Rawlings ND, Barrett AJ (1991) Homologues of insulinase, a new superfamily of metalloendopeptidases. Biochem J 275:389–391.
61. Becker AB, Roth RA (1992) An unusual active site identified in a family of zinc metalloendopeptidases. Proc Natl Acad Sci USA 89:3835–3839.
62. Maruyama Y, Chuma A, Mikami B, Hashimoto W, Murata K (2011) Heterosubunit composition and crystal structures of a novel bacterial M16B metallopeptidase. J Mol Biol 407:180–192.
63. Matthews BW (1988) Structural basis of the action of thermolysin and related zinc peptidases. Acc Chem Res 21:333–340.
64. Polgár L. Basic kinetic mechanisms of proteolytic enzymes. In: Sterchi EE, Stöcker W, Eds. (1999) Proteolytic enzymes—Tools and targets. Berlin/Heidelberg: Springer Verlag, pp 148–166.
65. Schechter I, Berger A (1967) On the size of active site in proteases. I. Papain. Biochem Biophys Res Commun 27:157–162.
66. Timmer JC, Zhu W, Pop C, Regan T, Snipas SJ, Eroshkin AM, Riedl SJ, Salvesen GS (2009) Structural and kinetic determinants of protease substrates. Nat Struct Mol Biol 16:1101–1108.
67. Madala PK, Tyndall JDA, Nall T, Fairlie DP (2010) Update 1: proteases universally recognize beta strands in their active sites. Chem Rev 110:PR1–PR31.
68. Vallee BL, Neurath H (1954) Carboxypeptidase, a zinc metalloprotein. J Am Chem Soc 76:5006.
69. Vallee BL, Auld DS (1990) Zinc coordination, function, and structure of zinc enzymes and other proteins. Biochemistry 29:5647–5659.
70. Vallee BL, Auld DS (1990) Active-site zinc ligands and activated H2O of zinc enzymes. Proc Natl Acad Sci USA 87:220–224.
71. Lipscomb WN, Hartsuck JA, Reeke Jr. GN, Quiocho FA, Bethge PH, Ludwig ML, Steitz TA, Muirhead H, Coppola JC (1968) The structure of carboxypeptidase A. VII. The 2.0-Å resolution studies of the enzyme and of its complex with glycyltyrosine, and mechanistic deductions. Brookhaven Symp Biol 21:24–90.
72. Matthews BW, Jansonius JN, Colman PM, Schoenborn BP, Dupourque D (1972) Three-dimensional structure of thermolysin. Nature 238:37–41.
73. Pelmenschikov V, Siegbahn PEM (2002) Catalytic mechanism of matrix metalloproteinases: two-layered ONIOM study. Inorg Chem 41:5659–5666.
74. Bertini I, Calderone V, Fragai M, Luchinat C, Maletta M, Yeo KJ (2006) Snapshots of the reaction mechanism of matrix metalloproteinases. Angew Chem Int Ed Engl 45:7952–7955.
75. Bode W, Gomis-Rüth FX, Huber R, Zwilling R, Stöcker W (1992) Structure of astacin and implications for activation of astacins and zinc-ligation of collagenases. Nature 358:164–167.
76. Gomis-Rüth FX, Kress LF, Bode W (1993) First structure of a snake venom metalloproteinase: a prototype for matrix metalloproteinases/collagenases. EMBO J 12:4151–4157.
77. Kilshtain-Vardi A, Glick M, Greenblatt HM, Goldblum A, Shoham G (2003) Refined structure of bovine carboxypeptidase A at 1.25 Å resolution. Acta Cryst D59: 323–333.
78. Jongeneel CV, Bouvier J, Bairoch A (1989) A unique signature identifies a family of zinc-dependent metallopeptidases. FEBS Lett 242:211–214.
79. McKerrow JH (1987) Human fibroblast collagenase contains an amino acid sequence homologous to the zinc-binding site of Serratia protease. J Biol Chem 262:5943–5943.
80. Feng L, Yan H, Wu Z, Yan N, Wang Z, Jeffrey PD, Shi Y (2007) Structure of a site-2 protease family intramembrane metalloprotease. Science 318:1608–1612.
81. Fushimi N, Ee CE, Nakajima T, Ichishima E (1999) Aspzincin, a family of metalloendopeptidases with a new zinc-binding motif. Identification of new zinc-binding sites (His(128), His(132), and Asp(164)) and three catalytically crucial residues (Glu(129), Asp(143), and Tyr(106)) of deuterolysin from Aspergillus oryzae by site-directed mutagenesis. J Biol Chem 274:24195–24201.
82. Hori T, Kumasaka T, Yamamoto M, Nonaka N, Tanaka N, Hashimoto Y, Ueki U, Takio K (2001) Structure of a new 'aspzincin' metalloendopeptidase from Grifola frondosa: implications for the catalytic mechanism and substrate specificity based on several different crystal forms. Acta Cryst D57:361–368.
83. McAuley KE, Jia-Xing Y, Dodson EJ, Lehmbeck J, Ostergaard PR, Wilson KS (2001) A quick solution: ab initio structure determination of a 19 kDa metalloproteinase using ACORN. Acta Cryst D57:1571–1578.
84. Bieniossek C, Schalch T, Bumann M, Meister M, Meier R, Baumann U (2006) The molecular architecture of the metalloprotease FtsH. Proc Natl Acad Sci USA 103:3066–3071.
85. Suno R, Niwa H, Tsuchiya D, Zhang X, Yoshida M, Morikawa K (2006) Structure of the whole cytosolic region of ATP-dependent protease FtsH. Mol Cell 22: 575–585.
86. Bieniossek C, Niederhauser B, Baumann UM (2009) The crystal structure of apo-FtsH reveals domain movements necessary for substrate unfolding and translocation. Proc Natl Acad Sci USA 106:21579–21584.
87. Langklotz S, Baumann U, Narberhaus F (2012) Structure and function of the bacterial AAA protease FtsH. Biochim Biophys Acta 1823:40–48.
88. López-Pelegrín M, Cerdà-Costa N, Martínez-Jiménez F, Cintas-Pedrola A, Canals A, Peinado JR, Martí-Renom MA, López-Otín C, Arolas JL, Gomis-Rüth FX (2013) A novel family of soluble minimal scaffolds

provides structural insight into the catalytic domains of integral-membrane metallopeptidases. J Biol Chem 288:21279–21294.
89. Montecucco C, Schiavo G (1993) Tetanus and botulism neurotoxins: a new group of zinc proteases. Trends Biochem Sci 18:324–327.
90. Swaminathan S (2011) Molecular structures and functional relationships in clostridial neurotoxins. FEBS J 278:4467–4485.
91. Tronrud DE, Roderick SL, Matthews BW (1992) Structural basis for the action of thermolysin. Matrix 1:107–111.
92. Adekoya OA, Sylte I (2009) The thermolysin family (M4) of enzymes: therapeutic and biotechnological potential. Chem Biol Drug Des 73:7–16.
93. Eijsink VG, Matthews BW, Vriend G (2011) The role of calcium ions in the stability and instability of a thermolysin-like protease. Prot Sci 20:1346–1355.
94. Pannifer AD, Wong TY, Schwarzenbacher R, Renatus M, Petosa C, Bienkowska J, Lacy DB, Collier RJ, Park S, Leppla SH, Hanna P, Liddington RC (2001) Crystal structure of the anthrax lethal factor. Nature 414:229–233.
95. Xu Q, Gohler AK, Kosfeld A, Carlton D, Chiu HJ, Klock HE, Knuth MW, Miller MD, Elsliger MA, Deacon AM, Godzik A, Lesley SA, Jahreis K, Wilson IA (2012) The structure of Mlc titration factor A (MtfA/YeeI) reveals a prototypical zinc metallopeptidase related to anthrax lethal factor. J Bacteriol 194: 2987–2999.
96. Pryor EE, Jr., Horanyi PS, Clark KM, Fedoriw N, Connelly SM, Koszelak-Rosenblum M, Zhu G, Malkowski MG, Wiener MC, Dumont ME (2013) Structure of the integral membrane protein CAAX protease Ste24p. Science 339:1600–1604.
97. Quigley A, Dong YY, Pike AC, Dong L, Shrestha L, Berridge G, Stansfeld PJ, Sansom MS, Edwards AM, Bountra C, von Delft F, Bullock AN, Burgess-Brown NA, Carpenter EP (2013) The structural basis of ZMPSTE24-dependent laminopathies. Science 339: 1604–1607.
98. Kyrieleis OJ, Goettig P, Kiefersauer R, Huber R, Brandstetter H (2005) Crystal structures of the tricorn interacting factor F3 from Thermoplasma acidophilum, a zinc aminopeptidase in three different conformations. J Mol Biol 349:787–800.
99. Addlagatta A, Gay L, Matthews BW (2006) Structure of aminopeptidase N from Escherichia coli suggests a compartmentalized, gated active site. Proc Natl Acad Sci USA 103:13339–13344.
100. Tholander F, Muroya A, Roques BP, Fournie-Zaluski MC, Thunnissen MM, Haeggstrom JZ (2008) Structure-based dissection of the active site chemistry of leukotriene A4 hydrolase: implications for M1 aminopeptidases and inhibitor design. Chem Biol 15:920–929.
101. Eckhard U, Schonauer E, Nuss D, Brandstetter H (2011) Structure of collagenase G reveals a chew-and-digest mechanism of bacterial collagenolysis. Nat Struct Mol Biol 18:1109–1114.
102. Eckhard U, Schonauer E, Brandstetter H (2013) Structural basis for activity regulation and substrate preference of clostridial collagenases G, H, and T. J Biol Chem 288:20184–20194.
103. Oefner C, D'Arcy A, Hennig M, Winkler FK, Dale GE (2000) Structure of human neutral endopeptidase (Neprilysin) complexed with phosphoramidon. J Mol Biol 296:341–349.
104. Bland ND, Pinney JW, Thomas JE, Turner AJ, Isaac RE (2008) Bioinformatic analysis of the neprilysin (M13) family of peptidases reveals complex evolutionary and functional relationships. BMC Evol Biol 8:16.
105. Baral PK, Jajcanin-Jozic N, Deller S, Macheroux P, Abramic M, Gruber K (2008) The first structure of dipeptidyl-peptidase III provides insight into the catalytic mechanism and mode of substrate binding. J Biol Chem 283:22316–22324.
106. Yeh DC, Parsons LM, Parsons JF, Liu F, Eisenstein E, Orban J (2005) NMR structure of HI0004, a putative essential gene product from Haemophilus influenzae, and comparison with the X-ray structure of an Aquifex aeolicus homolog. Prot Sci 14:424–430.
107. Penhoat CH, Li Z, Atreya HS, Kim S, Yee A, Xiao R, Murray D, Arrowsmith CH, Szyperski T (2005) NMR solution structure of Thermotoga maritima protein TM1509 reveals a Zn-metalloprotease-like tertiary structure. J Struct Funct Genom 6:51–62.
108. Oganesyan V, Busso D, Brandsen J, Chen S, Jancarik J, Kim R, Kim SH (2003) Structure of the hypothetical protein AQ_1354 from Aquifex aeolicus. Acta Cryst D59:1219–1223.
109. Jacob AI, Kohrer C, Davies BW, RajBhandary UL, Walker GC (2013) Conserved bacterial RNase YbeY plays key roles in 70S ribosome quality control and 16S rRNA maturation. Mol Cell 49:427–438.
110. Zhan C, Fedorov EV, Shi W, Ramagopal UA, Thirumuruhan R, Manjasetty BA, Almo SC, Fiser A, Chance MR, Fedorov AA (2005) The ybeY protein from Escherichia coli is a metalloprotein. Acta Cryst F61:959–963.
111. Baumann U, Wu S, Flaherty KM, McKay DB (1993) Three-dimensional structure of the alkaline protease of Pseudomonas aeruginosa: A two-domain protein with a calcium binding parallel beta roll motif. EMBO J 12:3357–3364.
112. Bode W, Reinemer P, Huber R, Kleine T, Schnierer S, Tschesche H (1994) The X-ray crystal structure of the catalytic domain of human neutrophil collagenase inhibited by a substrate analogue reveals the essentials for catalysis and specificity. EMBO J 13:1263–1269.
113. Kurisu G, Kinoshita T, Sugimoto A, Nagara A, Kai Y, Kasai N, Harada S (1997) Structure of the zinc endoprotease from Streptomyces caespitosus. J Biochem 121:304–308.
114. Schlagenhauf E, Etges R, Metcalf P (1998) The crystal structure of the Leishmania major surface proteinase leishmanolysin (gp63). Structure 6:1035–1046.
115. Díaz-Perales A, Quesada V, Peinado JR, Ugalde AP, Alvarez J, Suarez MF, Gomis-Rüth FX, López-Otín C (2005) Identification and characterization of human archaemetzincin-1 and −2, two novel members of a family of metalloproteases widely distributed in Archaea. J Biol Chem 280:30367–30375.
116. Tallant C, García-Castellanos R, Seco J, Baumann U, Gomis-Rüth FX (2006) Molecular analysis of ulilysin, the structural prototype of a new family of metzincin metalloproteases. J Biol Chem 281:17920–17928.
117. Goulas T, Arolas JL, Gomis-Rüth FX (2010) Structure, function and latency regulation of a bacterial enterotoxin potentially derived from a mammalian adamalysin/ADAM xenolog. Proc Natl Acad Sci USA 108: 1856–1861.
118. Waltersperger S, Widmer C, Wang M, Baumann U (2010) Crystal structure of archaemetzincin AmzA from Methanopyrus kandleri at 1.5 Å resolution. Proteins 78:2720–2723.

119. Graef C, Schacherl M, Waltersperger S, Baumann U (2012) Crystal structures of archaemetzincin reveal a moldable substrate-binding site. PloS One 7:e43863.
120. Yu AC, Worrall LJ, Strynadka NC (2012) Structural insight into the bacterial mucinase StcE essential to adhesion and immune evasion during enterohemorrhagic E. coli infection. Structure 20:707–717.
121. Ng NM, Littler DR, Paton AW, Le Nours J, Rossjohn J, Paton JC, Beddoe T (2013) EcxAB is a founding member of a new family of metalloprotease AB toxins with a hybrid cholera-like B subunit. Structure 21: 2003–2013.
122. Maskos K, Bode W (2003) Structural basis of matrix metalloproteinases and tissue inhibitors of metalloproteinases. Mol Biotechnol 25:241–266.
123. Pieper M, Betz M, Budiša N, Gomis-Rüth FX, Bode W, Tschesche H (1997) Expression, purification, characterization, and X-ray analysis of selenomethionine 215 variant of leukocyte collagenase. J Prot Chem 16: 637–650.
124. Boldt HB, Overgaard MT, Laursen LS, Weyer K, Sottrup-Jensen L, Oxvig C (2001) Mutational analysis of the proteolytic domain of pregnancy-associated plasma protein-A (PAPP-A): classification as a metzincin. Biochem J 358:359–367.
125. Hege T, Baumann U (2001) The conserved methionine residue of the metzincins: a site-directed mutagenesis study. J Mol Biol 314:181–186.
126. Butler GS, Tam EM, Overall CM (2004) The canonical methionine 392 of matrix metalloproteinase 2 (gelatinase A) is not required for catalytic efficiency or structural integrity: probing the role of the methionine-turn in the metzincin metalloprotease superfamily. J Biol Chem 279:15615–15620.
127. Perez L, Kerrigan JE, Li X, Fan H (2007) Substitution of methionine 435 with leucine, isoleucine, and serine in tumor necrosis factor α converting enzyme inactivates ectodomain shedding activity. Biochem Cell Biol 85:141–149.
128. Oberholzer AE, Bumann M, Hege T, Russo S, Baumann U (2009) The metzincin's canonical methionine is responsible for the structural integrity of the zinc-binding site. Biol Chem 390:875–881.
129. Tallant C, García-Castellanos R, Baumann U, Gomis-Rüth FX (2010) On the relevance of the Met-turn methionine in metzincins. J Biol Chem 285:13951–13957.
130. Tallant C, García-Castellanos R, Marrero A, Canals F, Yang Y, Reymond JL, Solà M, Baumann U, Gomis-Rüth FX (2007) Activity of ulilysin, an archaeal PAPP-A-related gelatinase and IGFBP protease. Biol Chem 388:1243–1253.
131. Grams F, Dive V, Yiotakis A, Yiallouros I, Vassiliou S, Zwilling R, Bode W, Stöcker W (1996) Structure of astacin with a transition-state analogue inhibitor. Nat Struct Biol 3:671–675.
132. Yiallouros I, Grosse-Berkhoff E, Stöcker W (2000) The roles of Glu93 and Tyr149 in astacin-like zinc peptidases. FEBS Lett 484:224–228.
133. Hege T, Baumann U (2001) Protease C of Erwinia chrysanthemi: the crystal structure and role of amino acids Y228 and E189. J Mol Biol 314:187–193.
134. Gomis-Rüth FX, Stöcker W, Huber R, Zwilling R, Bode W (1993) Refined 1.8 Å X-ray crystal structure of astacin, a zinc-endopeptidase from the crayfish Astacus astacus L. Structure determination, refinement, molecular structure and comparison with thermolysin. J Mol Biol 229:945–968.
135. Gomis-Rüth FX, Trillo-Muyo S, Stöcker W (2012) Functional and structural insights into astacin metallopeptidases. Biol Chem 393:1027–1041.
136. Guevara T, Yiallouros I, Kappelhoff R, Bissdorf S, Stöcker W, Gomis-Rüth FX (2010) Proenzyme structure and activation of astacin metallopeptidase. J Biol Chem 285:13958–13965.
137. Stöcker W, Gomis-Rüth FX, Bode W, Zwilling R (1993) Implications of the three-dimensional structure of astacin for the structure and function of the astacin-family of zinc-endopeptidases. Eur J Biochem 214: 215–231.
138. Bond JS, Beynon RJ (1995) The astacin family of metalloendopeptidases. Prot Sci 4:1247–1261.
139. Zwilling R, Stöcker W (1997) The astacins—Structure and function of a new protein family. Naturwissenschaftliche Forschungsergebnisse. Hamburg (Germany): Verlag Dr. Kovač, pp 370.
140. Villa JP, Bertenshaw GP, Bylander JE, Bond JS (2003) Meprin proteolytic complexes at the cell surface and in extracellular spaces. In: The Biochemical Society Symposium, pp 53–63.
141. Semenova SA, Rudenskaia GN (2008) The astacin family of metalloproteinases. Biomeditsinskaia khimiia 54:531–554.
142. Sterchi EE, Stöcker W, Bond JS (2008) Meprins, membrane-bound and secreted astacin metalloproteinases. Mol Aspects Med 29:309–328.
143. Maeda H, Morihara K (1995) Serralysin and related bacterial proteinases. Meth Enzymol 248:395–413.
144. Baumann U. Chapter 180—Serralysin and related enzymes. In: Rawlings ND, Salvesen GS, Eds. (2013) Handbook of proteolytic enzymes. Oxford: Academic Press, pp 864–867.
145. Morihara K (1957) Studies on the protease of Pseudomonas. II. Crystallization of the protease and its physicochemical and general properties. Bull Agric Chem Soc Jpn 21:11–17.
146. Morihara K, Homma JY. Pseudomonas proteases. In: Holder IA, Ed. (1985) Bacterial enzymes and virulence. Boca Ratón, FL: CRC Press, pp 41–79.
147. Baumann U (1994) Crystal structure of the 50 kDa metallo protease from Serratia marcescens. J Mol Biol 242:244–251.
148. Baumann U, Bauer M, Letoffe S, Delepelaire P, Wandersman C (1995) Crystal structure of a complex between Serratia marcescens metallo-protease and an inhibitor from Erwinia chrysanthemi. J Mol Biol 248: 653–661.
149. Hege T, Feltzer RE, Gray RD, Baumann U (2001) Crystal structure of a complex between Pseudomonas aeruginosa alkaline protease and its cognate inhibitor. Inhibition by a zinc-NH2 coordinative bond. J Biol Chem 276:35087–35092.
150. McHugh B, Krause SA, Yu B, Deans AM, Heasman S, McLaughlin P, Heck MM (2004) Invadolysin: a novel, conserved metalloprotease links mitotic structural rearrangements with cell migration. J Cell Biol 167: 673–686.
151. Trillo-Muyo S, Martínez-Rodríguez S, Arolas JL, Gomis-Rüth FX (2013) Mechanism of action of a Janus-faced single-domain protein inhibitor simultaneously targeting two peptidase classes. Chem Sci 4:791–797.
152. Kurisu G, Kai Y, Harada S (2000) Structure of the zinc-binding site in the crystal structure of a zinc endoprotease from Streptomyces caespitosus at 1 Å resolution. J Inorg Biochem 82:225–228.

153. Gross J, Lapière CM (1962) Collagenolytic activity in amphibian tissues: a tissue culture assay. Proc Natl Acad Sci USA 48:1014–1022.
154. Cerdà-Costa N, Guevara T, Karim AY, Ksiazek M, Nguyen KA, Arolas JL, Potempa J, Gomis-Rüth FX (2011) The structure of the catalytic domain of Tannerella forsythia karilysin reveals it is a bacterial xenologue of animal matrix metalloproteinases. Mol Microbiol 79:119–132.
155. Guevara T, Ksiazek M, Skottrup PD, Cerda-Costa N, Trillo-Muyo S, de Diego I, Riise E, Potempa J, Gomis-Ruth FX (2013) Structure of the catalytic domain of the Tannerella forsythia matrix metallopeptidase karilysin in complex with a tetrapeptidic inhibitor. Acta Cryst F69:472–476.
156. McCawley LJ, Matrisian LM (2001) Matrix metalloproteinases: they're not just for matrix anymore! Curr Opin Cell Biol 13:534–540.
157. Nagase H, Woessner Jr. JF (1999) Matrix metalloproteinases. J Biol Chem 274:21491–21494.
158. Tallant C, Marrero A, Gomis-Rüth FX (2010) Matrix metalloproteinases: fold and function of their catalytic domains. Biochim Biophys Acta Mol Cell Res 1803: 20–28.
159. Puente XS, Sánchez LM, Overall CM, López-Otín C (2003) Human and mouse proteases: a comparative genomic approach. Nat Rev Genet 4:544–558.
160. Springman EB, Angleton EL, Birkedal-Hansen H, Van Wart HE (1990) Multiple modes of activation of latent human fibroblast collagenase: evidence for the role of a Cys73 active-site zinc complex in latency and a "cysteine switch" mechanism for activation. Proc Natl Acad Sci USA 87:364–368.
161. van Wart HE, Birkedal-Hansen H (1990) The cysteine switch: a principle of regulation of metalloproteinase activity with potential applicability to the entire matrix metalloproteinase gene family. Proc Natl Acad Sci USA 87:5578–5582.
162. Nagase H (1997) Activation mechanisms of matrix metalloproteinases. Biol Chem 378:151–160.
163. Woessner JF, Jr., Nagase H Matrix metalloproteinases and TIMPs. In: P. Sheterline, Ed. (2000) Protein profile series. New York: Oxford University Press.
164. Clark IM. Matrix metalloproteinase protocols. In: Walker JM, Ed. (2001) Methods in molecular biology. Totowa, NJ: Humana Press Inc., pp 545.
165. Visse R, Nagase H (2003) Matrix metalloproteinases and tissue inhibitors of metalloproteinases: structure, function, and biochemistry. Circ Res 92:827–839.
166. Murphy G, Nagase H (2008) Progress in matrix metalloproteinase research. Mol Aspects Med 29:290–308.
167. Murphy G (2011) Tissue inhibitors of metalloproteinases. Genome Biol 12:233.
168. Knapinska A, Fields GB (2012) Chemical biology for understanding matrix metalloproteinase function. Chembiochem 13:2002–2020.
169. Oshiro N, Miyagi E (2012) Matrix metalloproteinases—Biology, functions and clinical implications. Protein biochemistry, synthesis, structure abd cellular functions. Hauppauge, NY: Nova Science Publishers Inc., pp 241.
170. Tocchi A, Parks WC (2013) Functional interactions between matrix metalloproteinases and glycosaminoglycans. FEBS J 280:2332–2341.
171. Fox JW, Bjarnasson JB (1995) Snake venom metalloendopeptidases: reprolysins. Meth Enzymol 248:345–368.
172. Schlondorff J, Blobel CP (1999) Metalloprotease-disintegrins: modular proteins capable of promoting cell-cell interactions and triggering signals by protein-ectodomain shedding. J Cell Sci 112:3603–3617.
173. Cal S, Obaya AJ, Llamazares M, Garabaya C, Quesada V, López-Otín C (2002) Cloning, expression analysis, and structural characterization of seven novel human ADAMTSs, a family of metalloproteinases with disintegrin and thrombospondin-1 domains. Gene 283:49–62.
174. Fox JW, Serrano SM (2005) Structural considerations of the snake venom metalloproteinases, key members of the M12 reprolysin family of metalloproteinases. Toxicon 45:969–985.
175. Hooper NM, Lendeckel U (2005) The ADAM family of proteases. Dordrecht, The Netherlands: Springer, pp 344.
176. Edwards DR, Handsley MM, Pennington CJ (2008) The ADAM metalloproteinases. Mol Aspects Med 29: 258–289.
177. Murphy G (2008) The ADAMs: signalling scissors in the tumour microenvironment. Nat Rev Cancer 8: 929–941.
178. Apte SS (2009) A disintegrin-like and metalloprotease (reprolysin-type) with thrombospondin type 1 motif (ADAMTS) superfamily: functions and mechanisms. J Biol Chem 284:31493–31497.
179. Takeda S (2009) Three-dimensional domain architecture of the ADAM family proteinases. Semin Cell Dev Biol 20:146–152.
180. Klein T, Bischoff R (2011) Active metalloproteases of the A disintegrin and metalloprotease (ADAM) family: Biological function and structure. J Proteome Res 10: 17–33.
181. Le Goff C, Cormier-Daire V (2011) The ADAMTS(L) family and human genetic disorders. Human Mol Genet 20:R163–167.
182. Weber S, Saftig P (2012) Ectodomain shedding and ADAMs in development. Development 139:3693–3709.
183. Lund J, Olsen OH, Sorensen ES, Stennicke HR, Petersen HH, Overgaard MT (2013) ADAMDEC1 is a metzincin metalloprotease with dampened proteolytic activity. J Biol Chem 288:21367–21375.
184. Zhu GZ, Lin Y, Myles DG, Primakoff P (1999) Identification of four novel ADAMs with potential roles in spermatogenesis and fertilization. Gene 234:227–237.
185. Nagase H, Fushimi K (2008) Elucidating the function of noncatalytic domains of collagenases and aggrecanases. Connect Tissue Res 49:169–174.
186. Grams F, Huber R, Kress LF, Moroder L, Bode W (1993) Activation of snake venom metalloproteinases by a cysteine switch-like mechanism. FEBS Lett 335: 76–80.
187. Gomis-Rüth FX, Kress LF, Kellermann J, Mayr I, Lee X, Huber R, Bode W (1994) Refined 2.0Å X-ray crystal structure of the zinc-endopeptidase adamalysin II. Primary and tertiary structure determination, refinement, molecular structure and comparison with astacin, collagenase and thermolysin. J Mol Biol 239:513–544.
188. Cirilli M, Gallina C, Gavuzzo E, Giordano C, Gomis-Rüth FX, Gorini B, Kress LF, Mazza F, PaglialungaParadisi M, Pochetti G, Politi V (1997) 2-Å X-ray structure of adamalysin II complexed with a peptide phosphonate inhibitor adopting a retro-binding mode. FEBS Lett 418:319–322.
189. Gomis-Rüth FX, Meyer EF, Kress LF, Politi V (1998) Structures of adamalysin II with peptidic inhibitors. Implications for the design of tumor necrosis factor α convertase inhibitors. Prot Sci 7:283–292.
190. Wisniewska M, Goettig P, Maskos K, Belouski E, Winters D, Hecht R, Black R, Bode W (2008)

Structural determinants of the ADAM inhibition by TIMP-3: crystal structure of the TACE-N-TIMP-3 complex. J Mol Biol 381:1307–1319.
191. Baumann U, Gomis-Rüth FX. Chapter 270—Ulilysin (*Methanosarcina acetivorans*). In: Rawlings ND, Salvesen G, Eds. (2013) Handbook of proteolytic enzymes. Oxford: Academic Press, pp 1208–1211.
192. García-Castellanos R, Tallant C, Marrero A, Solà M, Baumann U, Gomis-Rüth FX (2007) Substrate specificity of a metalloprotease of the pappalysin family revealed by an inhibitor and a product complex. Arch Biochem Biophys 457:57–72.
193. Kosowska K, Reinholdt J, Rasmussen LK, Sabat A, Potempa J, Kilian M, Poulsen K (2002) The Clostridium ramosum IgA proteinase represents a novel type of metalloendopeptidase. J Biol Chem 277:11987–11994.
194. Potempa J, Poulsen K. Chapter 274—The IgA protease of *Clostridium ramosum*. In: Rawlings ND, Salvesen G, Eds. (2013) Handbook of proteolytic enzymes. Oxford: Academic Press, pp 1225–1228.
195. Mulks MH, Shoberg RJ (1994) Bacterial immunoglobulin A1 proteases. Meth Enzymol 235:543–554.
196. Plaut AG, Qiu J. Chapter 278—IgA-specific metalloendopeptidase. In: Rawlings ND, Salvesen G, Eds. (2013) Handbook of proteolytic enzymes. Oxford: Academic Press, pp 1243–1248.
197. Merritt EA, Hol WG (1995) AB5 toxins. Curr Opin Struct Biol 5:165–171.
198. Beddoe T, Paton AW, Le Nours J, Rossjohn J, Paton JC (2010) Structure, biological functions and applications of the AB5 toxins. Trends Biochem Sci 35:411–418.
199. Gomis-Rüth FX (2013) A different look for AB5 toxins. Structure 21:1909–1910.
200. Myers LL, Firehammer BD, Shoop DS, Border MM (1984) Bacteroides fragilis: a possible cause of acute diarrheal disease in newborn lambs. Infect Immun 44:241–244.
201. Shiryaev SA, Remacle AG, Chernov AV, Golubkov VS, Motamedchaboki K, Muranaka N, Dambacher CM, Capek P, Kukreja M, Kozlov IA, Perucho M, Cieplak P, Strongin AY (2013) Substrate cleavage profiling suggests a distinct function of *Bacteroides fragilis* metalloproteinases (fragilysin and metalloproteinase II) at the microbiome-inflammation-cancer interface. J Biol Chem. doi: 10.1074/jbc.M113.516153.
202. Goulas T, Gomis-Rüth FX. 186. Fragilysin. In: Rawlings ND, Salvesen GS, Eds. (2013) Handbook of proteolytic enzymes. Oxford: Academic Press, pp 887–891.
203. Karaolis DKR, Lan R, Kaper JB, Reeves PR (2001) Comparison of Vibrio cholerae pathogenicity islands in sixth and seventh pandemic strains. Infect Immun 69:1947–1952.
204. Szabady RL, Yanta JH, Halladin DK, Schofield MJ, Welch RA (2011) TagA is a secreted protease of Vibrio cholerae that specifically cleaves mucin glycoproteins. Microbiology 157:516–525.
205. Szabady RL, Welch RA. Chapter 286—StcE peptidase and the StcE-like metallopeptidases. In: Rawlings ND, Salvesen G, Eds. (2013) Handbook of proteolytic enzymes. Oxford: Academic Press, pp 1272–1280.
206. Lathem WW, Grys TE, Witowski SE, Torres AG, Kaper JB, Tarr PI, Welch RA (2002) StcE, a metalloprotease secreted by Escherichia coli O157:H7, specifically cleaves C1 esterase inhibitor. Molecul Microbiol 45:277–288.